UNIVERSITY OF TWENTE.

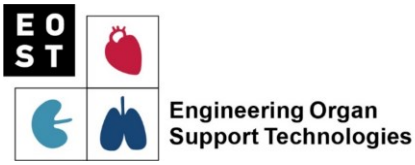

Faculty of Engineering Technology

Department of Biomechanical Engineering

Chair of Engineering Organ Support Technologies

Prof. Dr.-Ing. Jutta Arens

Development of a Neonatal Umbilical Cannulation Simulator: Design and User Validation

Submitted as	Master‘s Thesis
Name, student no.:	L.G. van der Woerd, S2157179
Date:	19 June 2024
Supervisor	Prof. Dr.-Ing. Jutta Arens
Daily Supervisor	ir. D.J.M van Galen
External committee member	Niels Rochow MD PhD
Internal committee member	Dr. Frank R. Halfwerk

Declaration

I hereby declare that I have written this thesis independently. Only the sources and aids expressly named in the thesis have been used. I have marked as such any ideas taken over verbatim or in spirit.

Enschede, 19 June 2024_____ 

Place, Date Signature

Preface or Acknowledgement

After 9 months of hard work and labour, I am proud to deliver the work that marks the completion of my studies for Biomedical Engineering. I have enjoyed my time at the EOST group and would specifically like to thank Jutta for the warm welcome. I would also like to thank her for the opportunity to gain experience on-site by allowing me to travel to Neurenberg (twice) and the introduction to Zwiebelkuchen und Federweißer. I would also like to thank Niels for showing me the Klinikum Nürnberg and helping me gain insight in the clinical side of the problem.

A special thanks in particular to all the neonatologists and paediatricians of the Klinikum Nürnberg and the German HeartCenter Munich participating in the survey and providing valuable feedback. Without them, the survey would be all questions, no answers.

Also, thank you Ana, for taking the time to give me an introduction for working with silicones, all the way from Italy.

I would also like to thank Frank for all the feedback provided along the way, but specifically the help in applying statistics to my results.

Finally, a thank you to Danny for the ability to always go to him with questions, but maybe as importantly, the simple act of just holding his employee pass in front of the coffee machine.

Please enjoy the reading of my findings,

Levien

Problem Definition

The ArtPlac project is developing an artificial placenta which should aid preterm neonates with providing dialysis and oxygenation support. An important part of the ArtPlac project is the development of a novel umbilical cannula. To develop such a device, a reference physical model of the neonates' venous tract is needed. This model should not only be used for development and testing of the cannula, but also for practicing the ultimate procedure. Currently no anatomically correct model with matching material properties is available. The materials that can be used to construct such a venous simulator have not been compared to the mechanical properties of human umbilical veins. They have also not been validated by neonatologists.

Abstract

Introduction Every year, 15 million preterm children are born worldwide, 10 % of whom are born before 31 weeks of gestation. The ArtPlac project aims to build a combined lung and kidney support system that can be connected through the umbilical cord using a specialized, yet to be developed, cannula. A surgical preterm neonatal surgical simulator is needed to aid in this development.

Aim The aim of this master's thesis is to identify realistic materials and production processes that can be used to develop vasculature models for use in a realistic neonatal cannulation simulator.

Methods Material choices for use in a cannulation simulator were evaluated. For creating veins, four silicones and two 3D-printable materials were considered. Tensile test results for Young's modulus, tensile strength and breaking strain were compared to values found in literature for human umbilical veins. Veins were produced from HT 33, Vascuflex, and Superflex, for further evaluation. These venous models were incorporated in preterm neonatal simulators together with materials mimicking the surrounding tissue and Wharton's Jelly. Neonatologists performed the simulated cannulation procedure on these simulators and provided feedback on the materials by means of a survey.

Results Mechanical testing showed that most materials matched at a low strain range (0 – 10 %) in terms of stiffness. None of the materials matched in all evaluated properties. According to the survey, more flexible materials were preferred, especially for the Wharton's jelly. Tensile strength and breaking strain did not seem to affect the simulator experience in terms of puncturing and tearing. Movement of the vein within the body was found to be imperceptible by participants.

Conclusion 3D-printing anatomically correct vasculature models using Superflex was found to be performing best in terms of haptic realism. To mimic Wharton's jelly, a more compliant material should be identified.

Keywords

Neonate, Surgical Simulator, Umbilical Cord, Umbilical Vein

Content

1 Introduction

Every year, an estimated 15 million preterm children are born worldwide [1], 10 % of whom are born between 28 and 31 gestational weeks (GA) [2]. Prior to 36 weeks, neonates are at increased risk for developing respiratory distress syndrome (RDS) and would need to be subjected to surfactant treatment[3]. Prior to 28 weeks, there may be no mature gas exchange surface available at all [3]. Development of the kidneys completes between 32 and 36 weeks [4]. These (very) preterm-born babies require support to finish organ maturation, such as ventilation or extracorporeal membrane oxygenation (ECMO) [2, 5].

The ArtPlac project [6], funded under The European Innovation Council (EIC, ID: 101099596), aims to be part of the solution for less invasive and higher-quality support of the neonate. It aims to develop a combined lung and kidney support system specifically designed for neonates rather than downscaling devices originally designed for adults. The ArtPlac project seeks to create a device with a singular interface connected to the neonate through its umbilical cord. The umbilical vessels will be preserved for the first weeks of life to ensure vascular access [6]. This greatly reduces the tubing necessary and thus the priming volume when compared to current treatment methods [6]. The cannulation procedure in order to keep the umbilical vessels open is yet to be developed.

Umbilical catheterization on its own is not a novel idea. Currently, it is used for the infusion of fluids or medication and for monitoring purposes only, using catheters of up to 5 Fr (1.66 mm in diameter) [7]. However, these catheters do not allow for oxygen and kidney support due to their flow restriction. To provide the necessary volume needed for oxygenation, high-flow cannulas of 10 Fr (3.33 mm in diameter) are necessary [6].

As umbilical cannulation using high-flow cannulas is a novel procedure, it will need to be preclinically validated in animals. The procedure has only been performed in animals at a handful of institutions and has not been used in neonatal care. To minimize the number of animal tests, as much of the testing as possible will be on in vitro models [6].

Current simulators for catheterization of the umbilical vein are based on real umbilical cords (UC) [8, 9]. Other neonatal simulators simply omit the UC [10, 11].

Currently, there is no long-term stable, off-the-shelf, and cost-effective synthetic simulator commercially available. Therefore, the aim of this master's thesis is to identify realistic materials that can be used to develop a realistic neonatal cannulation simulator.

2 Objectives

The objective of this research will be the search and validation of materials used for the construction of a surgical umbilical cannulation simulator. Main focus will be put towards the materials for the umbilical vein. Additionally, the materials for the surrounding tissue such as the umbilical cord as well as tissue that surround the veins within the body will also be included. The umbilical arteries will not be taken into account.

Main problems with a previously created simulator within the group were related to material properties and manufacturing techniques. The resulting model consisted of multiple separate 3D-printed parts printed using Vascuflex at 3D Medical Support (Enschede, the Netherlands). These were then combined with a silicone rubber compound. Both the material and the merging of the separate parts resulted in problems. The material ended up being too stiff, while the connection points became weak points which were prone to leaking.

Therefore, the main objective of this work is to identify and validate synthetic analogues to relevant biological tissues. This will be split up into **five** intermediate objectives.

Objective 1 – Obtaining biomechanical properties

The **first objective** will be determining biomechanical properties that might influence the haptic properties of the model. As the model will need to replicate the real human umbilical vein (HUV), finding out its mechanical properties is of utmost importance. This can then be used as a baseline for selecting different materials. This objective will be tackled by means of a literature review. Some hands-on experience with real human umbilical cords will also help in judging fidelity of prototypes.

Objective 2 – Selecting materials with similar properties

The **second objective** will be the selection of materials that inhibit mechanical properties in a similar range. This can be met by means of a literature review. Once a selection is made, the materials can be compared more precisely by performing the same mechanical testing as used for testing the HUV. Subjective realism of the chosen mechanical properties can be validated by asking clinical experts for their judgment through a survey.

Objective 3 – Obtaining a 3D model of a neonate's venous tract

The **third objective** will be creating a physical 3D model of the vasculature of a neonate with the selected materials. After obtaining a 3D dataset of a neonate, a production method can be defined based on the chosen materials. This includes the identification of different manufacturing processes that can be used to shape the material into the desired product.

Objective 4 – Surrounding tissue analogue

The **fourth objective** will be developing an analogue to the surrounding tissue of the vessels. This should allow for a realistic response in terms of movement/resistance of the veins when a cannula is inserted.

Objective 5 – Testing and validation

The **fifth objective** will be to build several simulators with different materials and perform validation testing with clinical experts to further narrow down the material choices. In combination with the results from the mechanical testing, a relation between mechanical properties and haptic realism can be construed.

3 Fundamentals and state of the art

Development of a realistic surgical simulator will require knowledge regarding anatomy, material science, and production techniques. These will be discussed in the following sections.

3.1 Anatomy

The left and right umbilical arteries are among the first to develop during the fourth week of gestation. Their initial connection with the dorsal aortae is already obliterated during the fifth week as they form a new connection with the iliac arteries [12]. As the walls of the arteries are muscular and elastin-rich, they rapidly constrict after the umbilical cord is cut off [13].

The development of the venous system starts in the third week after conception. This primitive system can be split up into three major components: the cardinal system, the vitelline veins and the umbilical vein [12]. The umbilical vein is of importance to the development of a simulator as this will be the entry point for the cannulation procedure.

During the first four weeks of gestation, two umbilical veins develop. A left and a right one. However, by week nine, the right vein will have already been obliterated completely. The left umbilical vein forms an anastomosis with the ductus venosus (DV), see Figure 3-1. The umbilical vein (UV) is the only vessel responsible for providing oxygenated blood to the foetus [12]. This makes the umbilical vein an oxygen-rich vessel, while the umbilical arteries are oxygen-poor contrary to most other veins and arteries.

After the umbilical cord enters the foetus through the navel, the umbilical vein diverges from the umbilical arteries. First passing over the intestine, close to the abdominal wall, then moving dorsally in the direction of the liver where it connects to the DV through the portal sinus [14]. The umbilical arteries pass the bladder inferiorly and then continue to their junction with the iliac arteries.

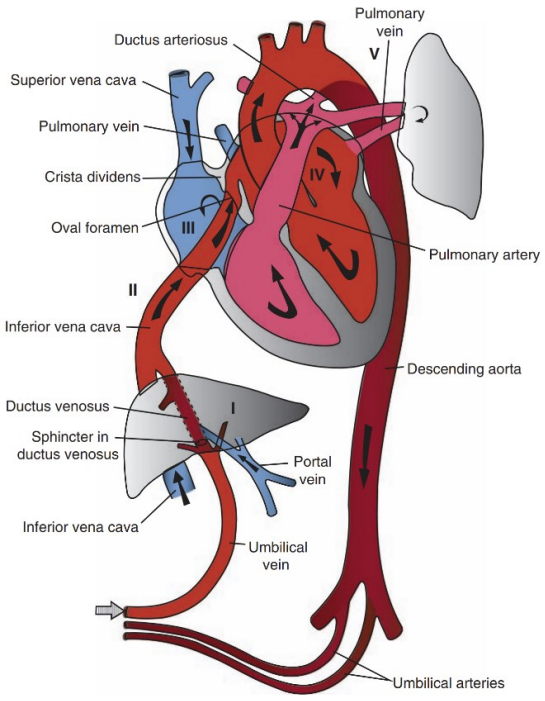

Figure 3-1: Foetal circulation before birth. Umbilical vein takes oxygen rich blood to the inferior vena cava and heart. Taken from [13].

The diameter of the umbilical vein and arteries grow with increasing gestational age, as the neonate requires higher blood flow rates. By a gestational age (GA) of 24 weeks, the internal diameter of the umbilical vein is around 6 mm. At birth (GA, 40) this will have grown to about 8.5 mm [15]. During the same period, the diameter of the arteries grows from 3.4 mm to 4.0 mm [15]. This parameter will be important for the ArtPlac project as it is needed to achieve enough flow for both oxygenation and kidney support. The chosen cannula will need to fit in the umbilical vein. Median wall thickness of the UV for healthy term births is 0.38 mm [16].

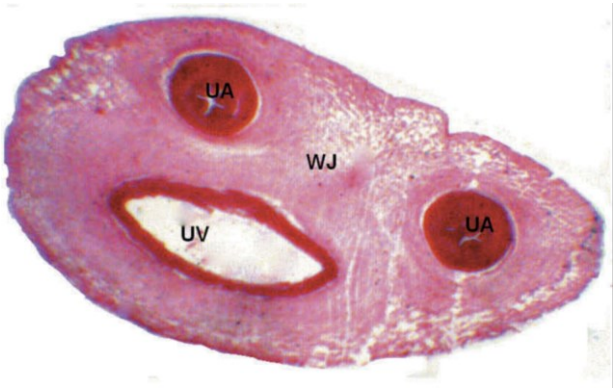

Figure 3-2: Cross section of a normal human umbilical cord. Two umbilical thick-walled arteries are indicated by **UA**. The umbilical vein is indicated with **UV**, featuring a much thinner wall. Adapted from [17].

Extracorporeally, these vessels are protected by a proteoglycan-rich tissue called Wharton's jelly [13]. The combined structure of the vessels and the Wharton's Jelly is called the umbilical cord (UC). For a cross-sectional cut of the UC, see Figure 3-2.

The UC guides the vein and two arteries to the placenta where nutrients, oxygen, and proteins are exchanged with maternal blood [12].

After turning into the DV, the UV connects with the vena cava (VC). This makes the VC the second vein of interest for building a simulator. The diameter of the VC at birth of term neonates is approximately 4.2 mm [18].

3.2 Material Science

A long-term usable simulator cannot be constructed out of real human umbilical veins as it would be subject to decomposition processes. Instead, a matching workable artificial material must be identified. This will be done by finding materials that closely match the mechanical properties of human umbilical veins. Taking into account flexibility and point of failure, the most interesting parameters are expected to be Young's modulus (E), ultimate strength, and breaking strain. As the materials to be used might behave non-linearly, multiple ways of obtaining a value for the Young's modulus can be utilized.

Values for E can be obtained through analysis of the linear section of the stress-strain curve or by approximation using an equation that relates hardness, which is quite easy to measure [19], to the Young's modulus.

3.2.1 Stiffness – hardness relation

A popular method of determining hardness of a material is the Shore A Hardness test. This test measures the distance of a spring-loaded indenter when pushed back under the force of the sample [19]. Although the value depends on the measured force and distance, the scale itself is dimensionless. The relation between force P in mN and the shore A hardness H_A value as stated by the ISO 48-4 [20] standard is specified as:

Equation 1: Force - Shore A relation

$$P = 550 + 75H_A$$

If the indenter is completely pushed back into the base, the reading of the Shore A hardness value will be 100. No pushback results in a Shore A hardness value of 0.

The efforts of Briscoe and Sebastian (1993) [19] have led to a relationship between H_A and E. They proposed the relation:

Equation 2: Shore A - Young's modulus relation

$$E = \frac{15.75+2.15H_A}{100 - H_A},$$

which relates Shora A hardness to Young's modulus.

3.2.2 General Overview Materials

To give a sense of the types of material that can be used to mimic the mechanical properties of veins, different types of materials were plotted based on strain and Young's modulus using Granta EduPack (Ansys GRANTA EduPack software, ANSYS, Inc., Cambridge, UK, 2023). Figure 3-3 shows a scatter-plot of common materials used in engineering, based on their elongation and Young's modulus. Plastics such as polypropylene and PVC are far too stiff. Materials that come close to venous tissue in terms of these mechanical properties are rubbers and silicones.

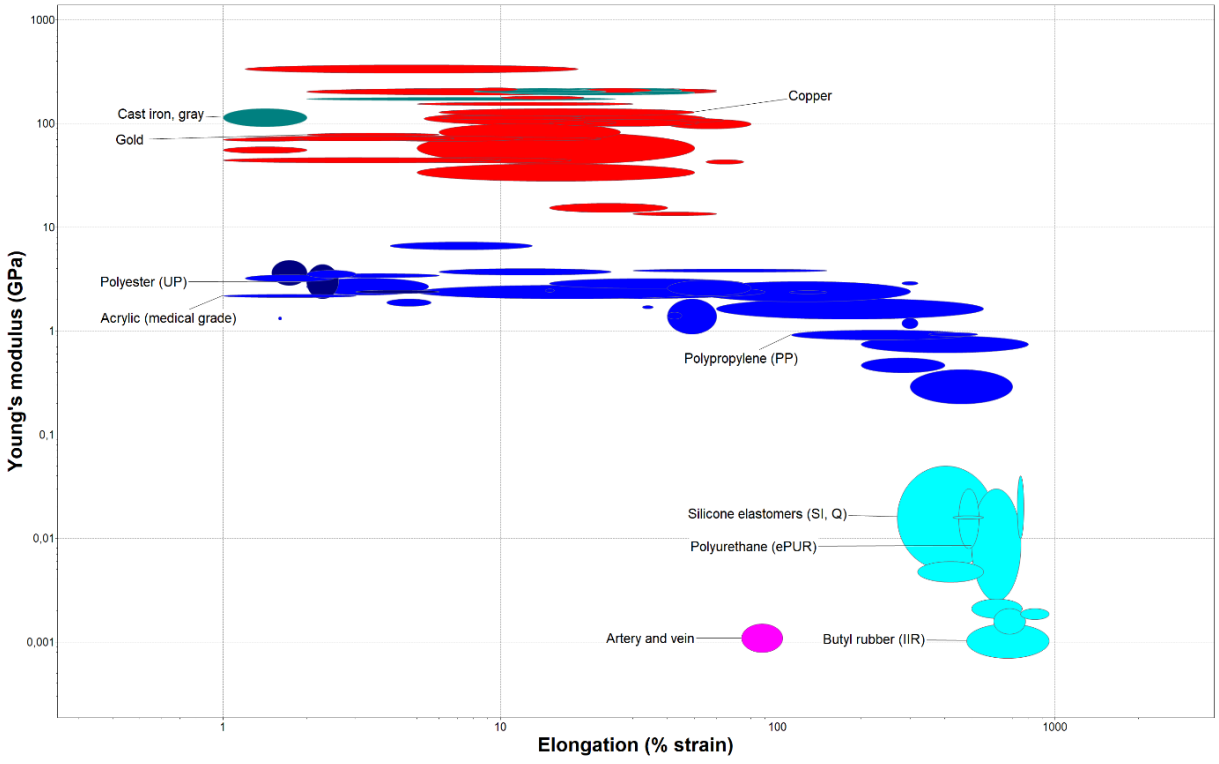

Figure 3-3: Material properties plotted based on their elongation and Young's modulus, created using Granta EduPack 2023 R2. **Red:** metals, **Dark Cyan:** ferrous metals, **Cyan:** Elastomers, **Magenta:** artery and vein.

3.3 Production Techniques

Producing an accurate, detailed and flexible 3D model of a small venous system is no trivial task. Major obstacles include reproducing wall thicknesses down to 0.38mm [16] as well as bifurcation points in the vessel structure. An obvious choice would be 3D printing for accurately reproducing a digital 3D model. However, each 3D printing principle is limited in its material choices. Table 3-1 shows widely available 3D printing principles as well as their relevance in reaching the goal of this project. For creating prototypes of non-3D-printable materials, other techniques such as moulding will be considered. Still, additive manufacturing will play a role even in alternative manufacturing techniques.

3.4 State of the Art

Simulation-based medical education (SBME) is the use of simulators as an alternative to real patients for educational purposes. These simulators can widely range in their form and function. They can be divided into four methods of simulation delivery: human patient simulators, task trainers, standardized patients, and virtual reality [21]. This research will have the goal of working towards a task trainer. A task trainer simulates only a part of the body and is meant to allow for repeated practice. They are generally cheaper than full human patient simulators but feature enough physiological fidelity in places where it matters [21]. The specific task for the task trainer to be developed is the insertion of a cannula (8 – 12 Fr) into the umbilical vein of the neonate up to the inferior vena cava. This should be achieved with realistic anatomy as well as realistic haptics concerning the umbilical vein, the Wharton's jelly, and the surrounding tissue.

3.4.1 Current Simulators

Previous simulators have been created using real umbilical cords attached to a mannequin through a bottle nipple [8], see Figure 3-4A. However, the use of this type of simulator is limited to hospitals, where UCs are easily and quickly obtainable. Long-term storage of this type of simulator poses challenges. It also limits training on UCs that are currently available, which will more often than not be UCs of term-neonates [22]. Early preterm births (<34 weeks) make up only 1-2 % of births [23], but are more relevant for training purposes regarding the ArtPlac project. Other neonatal ECMO simulators omit UV access or lack emulation of the heart [10]. Another umbilical-cannulation-specific simulator made use of an expensive simulator ($26,995 USD) with replaceable synthetic umbilical cords [24]. As a commercially available option, Premature Anne (Laerdal, Stavanger, Norway) can be purchased for $3,149 USD [25].

However, no link has been made between various material properties and their relevance to haptic realism.

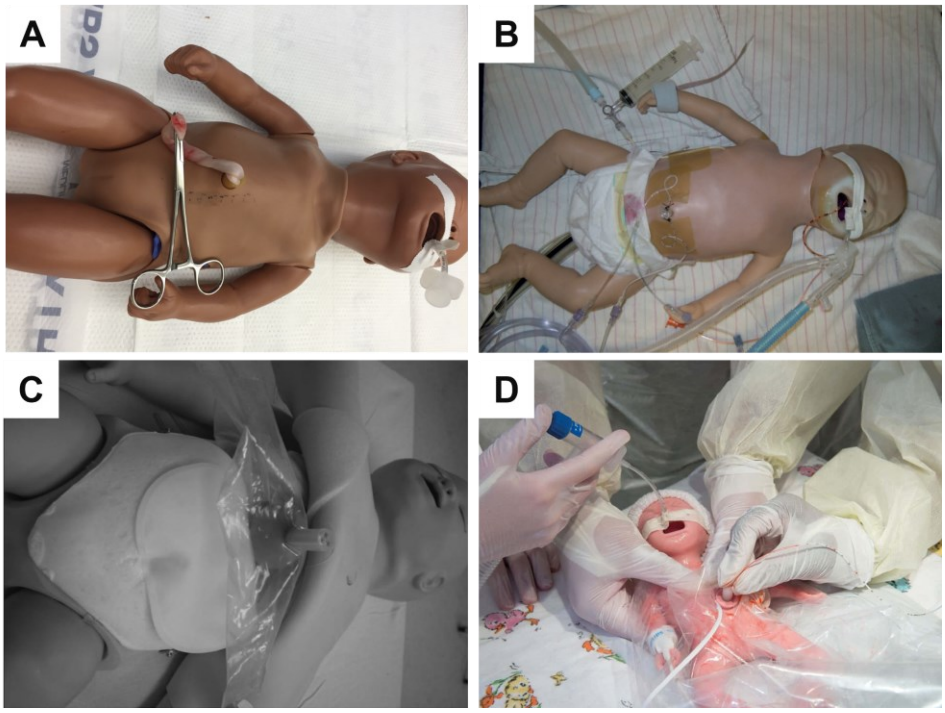

Figure 3-4: **A:** Simulator created using a real human umbilical vein [8], **B:** Neonatal ECMO cannulation simulator meant for training on carttid and jugular vessels [11], **C:** Modified Laerdal SimBaby to function as an Umbilical Cannulation task trainer [24], **C:** Commercialy available Laerdal Premature Anne [26].

Table 3-1: Working principle of widely available 3D-printing technologies and their advantages and disadvantages, as well as possible use case in the development of a simulator

Technique	Working principle	Resolution[1]	Advantages	Disadvantages	Possible use case
Fused Deposition modelling [27]	Material is heated to a temperature such that material turns plastic, then it is extruded through a nozzle. Subsequent layers are supported by previous layers	0.13 mm [27]	• Multiple material allows for dissolvable support [28] • Cheap material • Fast prints	• Without support; limited geometry • Limited to stiffer materials [27] • Low resolution	Quick iteration, mould creation, supporting components
Selective Laser Sintering [27]	A layer of powder is spread out after which a CO_2 laser bonds the powder together by sintering, grains are not fully fused together. Then a next layer of powder is deposited	0.08 mm [27]	• High precision possible (0.08mm) • No support needed	• Limited material choice • Expensive	Mould creation, supporting components
Vat polymerization [27]	A UV-light source is directed onto a thin layer of photosensitive polymer causing it to polymerize selectively. The source can be a UV laser (SLA) or a UV-emitting display (DLP). Printing often happens top-down as the model is lifted up from the vat.	0.025 mm [29]	• Allows for more flexible materials, down to 1.7 MPa at 100% strain [30] • High resolution, down to 0.025 mm[29]	• Without support; limited geometry • Smallest hole limited by viscosity of the unpolymerized polymer • 2-step procedure, full curing is done in an oven	Mould creation, final product
Silicone printing [31]	Two-component silicone is mixed in the nozzle and extruded out. Material remains in liquid form until after printing. The technique does depend on specific rheological properties, which limits silicone choice.	0.2 mm [32]	• Result in isotropic material	• 2-step procedure, crosslinking takes place after printing • Limited resolution of 0.35 mm layer height [31], or 0.2 mm nozzle size [32].	Printing final product

SLA = Stereolithography, DLP = Digital Light Processing, [1]Theoretical minimum feature size.

4 Materials and Methods

The main requirement of the simulator is mimicking the venous mechanical properties. Moreover, components should also be separate, quickly produced, and easily exchanged if damaged. The venous tract as well as other parts of the simulator, such as the umbilical cord and surrounding body, should be based on the anatomy of preterm neonates. For more information regarding requirements, see Annex F.

A selection of materials was collected based on material properties found in literature. Reference values for mechanical properties of umbilical veins were taken from Hamedani et al, 2012 [33]. They conducted mechanical testing on samples of umbilical veins which were collected after caesarean sections. A total of 3 HUV samples were tested. The mechanical properties are presented in Table 4-1.

Table 4-1: Reference values of mechanical properties HUV

Sample	Ultimate Tensile Strength (MPa)	E_{max} (MPa)[1]	$\varepsilon_{\_break}$ (%)
Longitudinal HUV	1.64 ± 0.11	7.35	33 ± 4
Circumferential HUV	0.97 ± 0.19	1.83	90 ± 16

[1]Calculated using the curve fitting coefficients as presented in the article

The graphs for the umbilical vein found in the article were digitized using Engauge Digitizer (Mark Mitchell, 2019, Version 12.1) to allow direct visual comparison with the measurements done on the collected materials. Average values and standard deviations for strength and strain were reproduced from the graphs.

Various materials were considered for comparison. Vascuflex and Superflex (3DMS, Enschede) were considered for their specific development for use in vascular models. The silicones HT 33 (Zhermack SpA, Badia Polesine), Dragon Skin 20 (DS 20) (Smooth-On, Macungie, Pennsylvania) , and RT 625 (Wacker Chemie AG, Munich) were considered for their flexibility and availability. RT 601 (Wacker Chemie AG, Munich) was considered for its tearing behaviour. Additionally, 3D-printable silicones such as SIL 001 (Lynxter [34]) and SIL 30 (Sandraw [35]) were considered but ultimately not included due to availability. These, among others, are presented in Annex H.

4.1 Mechanical Testing

Mechanical testing was performed according to the ISO 37 rubbers stress-strain testing protocol [36]. For HT 33, DS 20, RT 625, and RT 601, 2 mm thick slabs were casted. For both Vascuflex and Superflex, two 2 mm thick slabs were requested from 3DMS. One printed in the horizontal plane, and one printed in the vertical plane. This way, test pieces could be punched in different printing directions in order to test anisotropy as a result from the printing process.

From each sample, 5 test pieces were cut using an ISO 37 Type 2 cutting die. Similar to Hamedeni et al., testing was strain-controlled at a strain rate of 1 %/s. An overview of the different testing conditions is shown in Table 4-2. Testing was performed using a Zwick BZ1.0/TH1S (Zwick Roell, Ulm Germany).

As DS 20 showed diverging results during testing in terms of breaking strain and ultimate strength, the choice was made to include three extra test pieces for this material.

Three measurements of Shore A hardness were performed for each sample using a Zwick Roell durometer.

Two different tangent moduli were calculated for each material. The first is based on the first 10 % of elongation in order to compare initial elasticity. The second tangent modulus was based on the strain range for which the HUV behaves linearly in order to make a comparison to its Young's modulus. From each measurement, maximum values for both strain and strength were extracted for further analysis.

Following an insignificant Shapiro–Wilk test, values were compared to values of the HUV using the Student's *t*-test at a significance level of 5 %. A $p > 0.05$ means the results do not show significant difference, indicating they could be used as a synthetic substitute for a real HUV. To prevent type I errors, a Holm-Bonferroni correction was provided. Statistical analysis on the gathered data was performed using SPSS (IBM SPSS Statistics for Windows, Version 28.0.).

Table 4-2: Comparison between testing parameters

Sample	Strain rate	Test piece	Nr. of tests
Used method	1 %/s	ISO 37 type 2	5
Reference method [33]	1 %/s	custom	3

4.2 Obtaining a 3D model

An existing CT based adult 3D venous model [37] was used as a base for the neonates' venous tract. Iliac veins were deemed irrelevant and subsequently trimmed from the base model. Secondly, the model was scaled by 0.2x to match a 3D model of a neonate with a GA of 27 weeks in terms of scale. Trimming and scaling were done in SolidWorks 2023 (Dassault Systèmes SolidWorks Corp.).

A 3D model of an umbilical vein based on x-ray imaging, provided by Klinikum Nürnberg (Campus Süd), was combined with the scaled inferior vena cava of the previously mentioned model using Blender 3.4 (Blender foundation). More information regarding the process of scaling and combining the 3D model is available in Annex E.

4.3 Creating umbilical veins

Based on mechanical testing results, Vascuflex, Superflex, RT 601, and HT 33 were chosen for the creation of umbilical veins. Vascuflex and Superflex were chosen to compare 3D-printable materials. RT 601 and HT 33 were chosen to compare the impact breaking strain and UTS had on realism.

Various methods of fabrication for creating veins were considered. Prototypes for silicone veins were made using both coating and moulding procedures. For further information see Annex E.

Both an Ultimaker 3 (Ultimaker B.V., Geldermalsen) and a Bambu Lab X1C (Bambu Lab, Austin) were used for printing moulds. Moulds consisted of inner moulds, which determined the diameter of the lumen, and outer moulds, which determined the external diameter. All outer moulds were printed in PLA. For printing inner moulds, other materials were considered as well. For coating, only outer moulds were used. For more information regarding mould creation, see Annex A.

Directly 3D-printed veins were produced by 3DMS in both Vascuflex as well as Superflex using a vat polymerization printing process.

The veins were deemed watertight if water could traverse the vein without leaking along the way. Microscopy images were taken using a VHX 7000 (Keyence, Osaka) to determine the wall thickness of the resulting veins.

4.4 Surrounding tissue material

The function of the surrounding tissue is to support the veins within the body. The simulators should mimic the balance between support and ability for movement as it is in vivo, i.e. how it is supported by the intestines. The surrounding tissue and vein should be separate such that either are easily replaceable. Additionally, the material should be long-term stable and storable.

The following three materials were considered to mimic surrounding tissue. Konnyaku jelly was proposed by Tanigawa et al. [38], their main consideration was price, availability and ultrasound appearance. Secondly, Carbopol [39] was considered because it allows for vessel migration due to its granularity. Thirdly, water beads were considered, as this way veins could easily be replaced when necessary. Additionally, the size of the beads could be controlled by adding different amounts of water.

Based on Ease of Replacement, Cost of Replacement, Tunability, and Storability, materials were awarded between 1–3 points. A low score is assigned for Ease of Replacement if effort is needed to separate the surrounding tissue from other parts of the simulator, for example, if the material consists of a singular block. Cost of replacement is assigned a low score if it is more expensive. If the material is easily tuneable, for example in thickness or in size, a higher score is assigned. If the material consists of a liquid or of perishable goods, a lower score for Storability is awarded. Subjectively awarded points are presented in Table 4-3. Based on points awarded for these requirements, water beads were chosen for use in current prototypes.

Table 4-3: Points awarded to tissue-mimicking candidates based on the four criteria.

Mimicking material	Ease of replacement	Cost of Replacement	Tunability	Storability	Total
Konnyaku jelly	1	3	1	2	**8**
Carbopol	2	2	3	2	**9**
Water beads	3	3	3	2	**11**

To test maximum bead size, four beads were submerged in water for 48 hours after which they were measured using a calliper (Mitutoyo).

To determine the necessary ratio between water and beads for a certain diameter, twelve different conditions were created. Based on the value found for maximum bead size, 0.5 grams of beads were added to a range of 1–12 mL of water, with increments of 1 mL. After complete absorption,

three beads were taken for each condition and their diameter was measured using a calliper (Mitutoyo). The mean diameter was compared with the equation:

Equation 3: Expected relation between water content and resulting diameter

$$D_E = 2\sqrt[3]{\pi {r_{initial}}^3 + \frac{3}{4\pi} cx}\,,$$

in which $r_{initial}$ is the initial radius of the beads and c the volume increase per bead per mL added to 0.5 grams of beads. In this case $r_{initial}$ was 1 mm and c was 10.8. In Equation 3, x is the amount of water in mL added to 0.5 grams of beads.

Movement of the vein in the surrounding tissue upon insertion of a cannulation device was tested using a U-shaped silicone tube 15 cm in length. Three different insertion devices were inserted: a 4 Fr catheter, an 8 Fr cannula, and a guide wire. Movement was recorded with a camera and analysed using the Blender 3.4 Motion Tracking feature.

For mimicking Wharton's jelly, gelatine was considered because its stiffness could easily be controlled through varying water content. The vein was pulled through a piece of ½" silicone tubing and surrounded with liquid gelatine, then put in the fridge to solidify. Gelatine, however, was found to be lacking in strength. As an alternative, gummy bears were molten on a hotplate at 120 °C and watered down to decrease stiffness. This resulted in a more durable umbilical cord. More information regarding umbilical cord creation is available in Annex B.3.

4.5 Survey testing

Three materials for the veins were selected based on matching properties and producibility for further survey testing. Six simulators were built according to the method provided in Annex B. Two simulators were manufactured for each of the three different venous materials: Vascuflex, Superflex, and HT 33. RT 601 was excluded due to challenges with producibility. Each of the simulators was randomly awarded a name ranging from "Setup A" to "Setup F". These setups were presented to neonatologists and paediatricians from both Klinikum Nürnberg (Campus Süd) and the German HeartCenter Munich. Participants were asked to perform a cannulation procedure and provide answers to a questionnaire. The questionnaire consisted of ranking questions regarding material feel as well as Likert scale questions. For the questionnaire, see Annex C.

Responses to complementary Likert questions were aggregated into a unified score. Each response category was awarded a score: strongly disagree (−2), disagree (−1), agree (+1), strongly agree (+2). The overall score was obtained by subtracting the score of the negatively phrased question from its positively phrased counterpart.

In questions where participants were asked to rank the materials, the option for Real UV was included as well. This way, a value of distance to Real UV could be attributed to each material. A higher distance would mean that the material feels less like Real UV than a material with a lower distance, with regard to that specific question.

The analysis described above was done in Excel (Microsoft Corporation).

5 Results

5.1 Mechanical Testing

A Young's modulus of 8.05 ± 1.48 MPa was found from analysing the linear portion of longitudinal HUV from the work of Hamedani et al. [33]. The linear portion of the graph was found between 15 – 25 % strain. In case of the circumferential direction, E_{linear} was found to be 2.45 ± 1.11 MPa.

The resulting stress-strain graphs are presented in Figure 5-1. This shows a stark deviation in both ultimate strength as well as maximum strain for RT 625, HT 33 and DS 20 with respect to HUV.

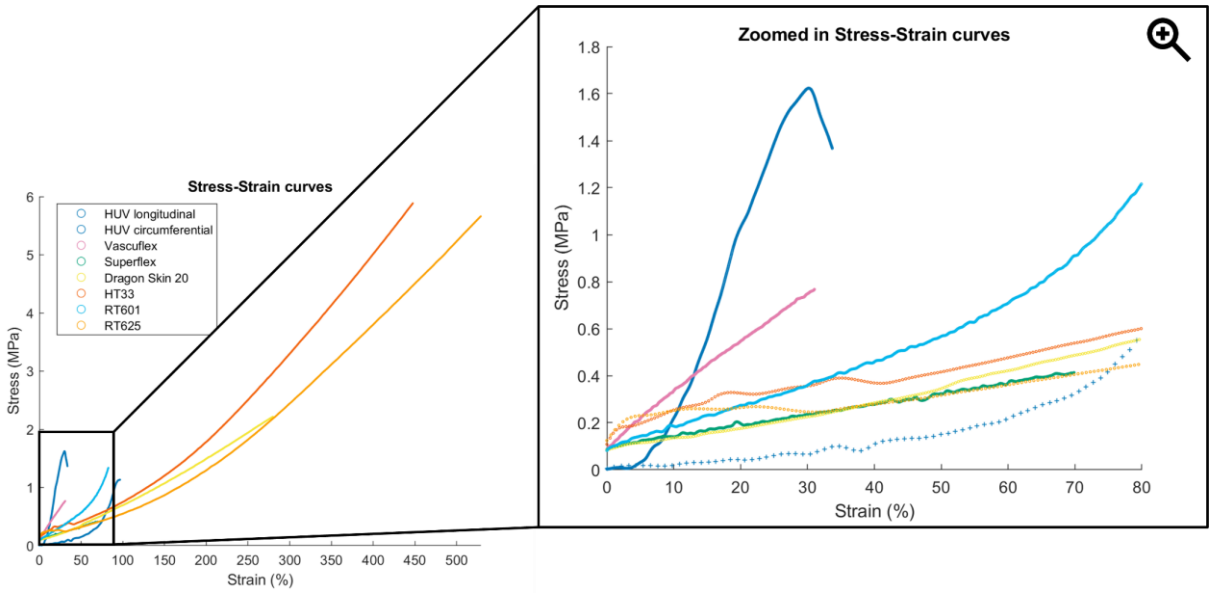

Figure 5-1: Stress-strain curves from the analysed materials. In dark-blue the reference data extracted from Hamedani et al. On the right is a zoomed-in graph at the 0 – 80 % strain range.

Neither Vascuflex nor Superflex showed significant differences between horizontal and vertical printing directions ($p > 0.05$). The presented data below (Figure 5-2) is for the vertical direction.

For further comparison of these parameters, mean and standard deviation for mechanical parameters are shown in Figure 5-2, p-values according to Student's *t*-test are presented after a Holm-Bonferroni correction. Taking $\alpha = 0.05$, significant differences with HUV are observed for ultimate strength and maximums strains, but not for both tangent moduli. Alternative p-values according to Mann-Whitney-U are presented in Annex G.

In case of the tangent modulus in the range 15 – 25 %, all p-values lie between 0.012 and 0.019 without Holm-Bonferroni correction. This correction leads to all p-values being > 0.05. For the

first 10 %, none of the materials behave significantly differently to HUV in terms of tangent modulus.

All materials differ significantly in terms of ultimate strength. In terms of maximum strain, only Vascuflex shows no statistical deviation from HUV measurements.

Values for Shore A hardness are presented in Table 5-1.

Table 5-1: Measured shore A hardnesses of the tested materials ordered from lowest to highest. Each Shore A was measured three times. Data are presented as mean ± std.

Sample	Shore A	Calculated $E_{shore\ A}$[1] (MPa)	E_{linear}[2] (MPa)
Superflex (3DMS)	15.1 ± 1.5	0.57 ± 0.05	0.43 ± 0.08[3]
DS 20	22.5 ± 0.6	0.83 ± 0.02	0.94 ± 0.02
RT 601	36.8 ± 0.7	1.50 ± 0.04	0.89 ± 0.03
HT 33	37.8 ± 2.4	1.56 ± 0.15	1.76 ± 0.06
RT 625	40.0 ± 1.5	1.70 ± 0.10	1.48 ± 0.09
Vascuflex (3DMS)	54.6 ± 0.9	2.93 ± 0.10	2.10 ± 0.06[3]

[1]Calculated using Equation 2. [2]Determined from the linear portion of the stress-strain curve. [3]Average and std taken are for all different measured directions (assumed isotropic).

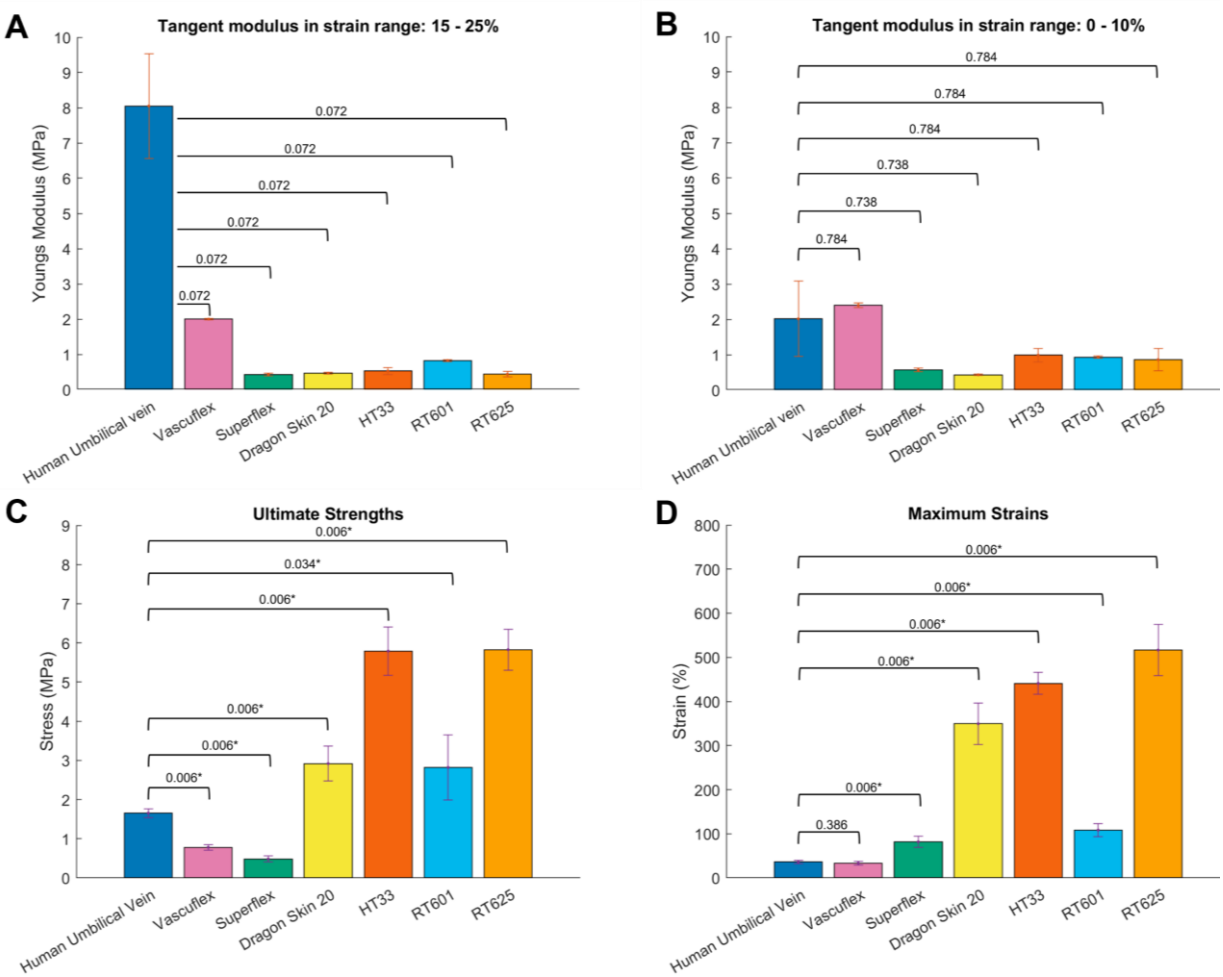

Figure 5-2: Bar charts containing mean and standard deviations from extracted mechanical parameters. p-values for the Student's *t*-test in comparison to HUV are indicated after the Holm-Bonferroni correction. * is used to indicate significant differences. **A:** Tangent moduli for the part where HUV behaves linearly. **B:** Tangent moduli on small strains. **C:** Ultimate strengths. **D:** Maximum strains.

At α = 0.05, Vascuflex differs non-significantly from HUV in three out of four parameters. All others only differ non-significantly in two parameters.

5.2 Obtaining a 3D model

The resulting 3D model of the venous tract is shown in Figure 5-3.

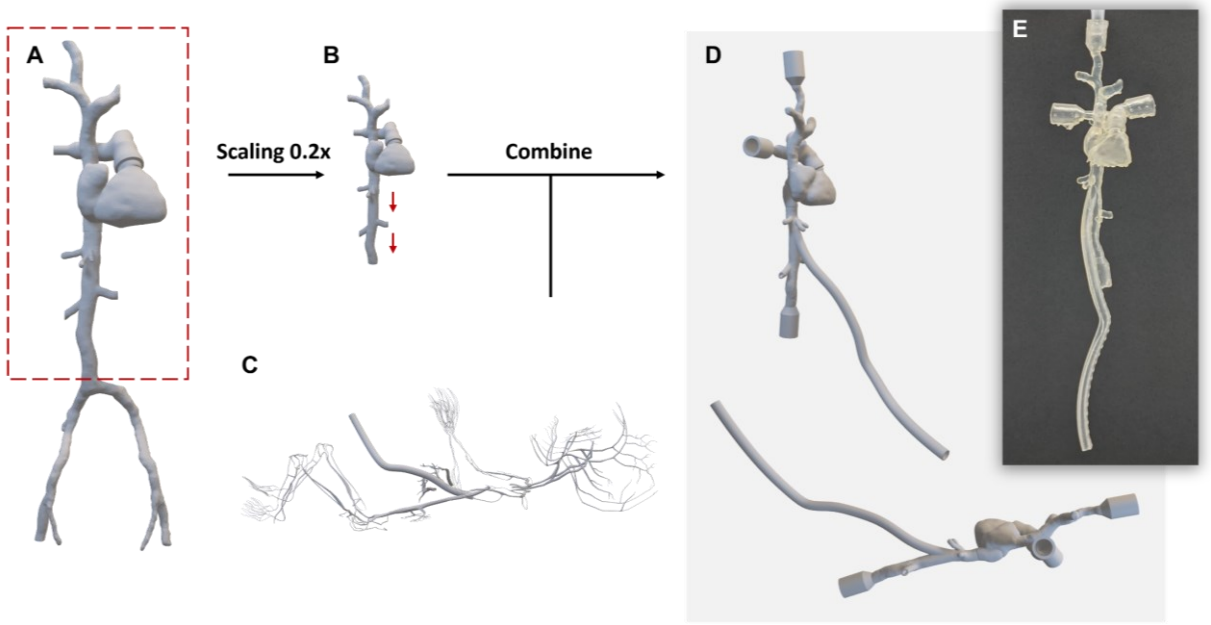

Figure 5-3: Resulting 3D model of the neonates' venous tract. **A:** Adult venous tract, red box represents region of interest, **B:** Scaled down model, lengthened in suprarenal and infrarenal portion of the vena cava (red arrows), **C:** Model provided by Klinikum Nürnberg, **D:** Combined model with added connectors (top: frontal view, bottom: lateral view), **E:** Physical 3D model as printed by 3DMS (Enschede, the Netherlands).

5.3 Creating umbilical veins

Experiences from vein creation are summarised in Table 5-2. Processes making use of inner moulds did not result in extractable veins. Microscopy images of slices from the veins in three different materials are shown in Figure 5-4. As is visible in Figure 5-4A, the lumen of Vascuflex veins is less circular and as a result smaller in area than Superflex (Figure 5-4C). Successfully extracted HT 33 veins had a standard deviation greater than 50 % of the average wall thickness, indicating high variability in thickness, this is also visible in Figure 5-4B.

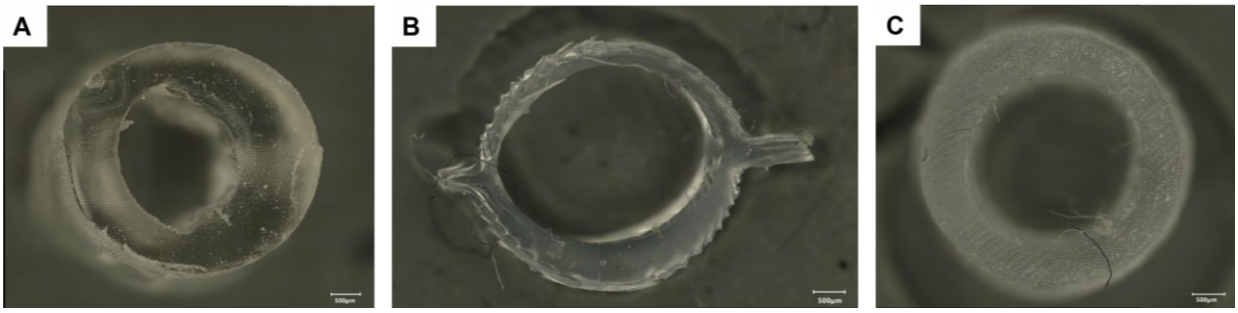

Figure 5-4: Microscopy imaging of circumferential slices of materials used for creating umbilical veins. **A:** Vascuflex, **B:** HT 33, **C:** Superflex. The scale bar at the bottom right represents 500 µm.

Table 5-2: Results and experiences from different materials and production techniques. y = Yes, n = No. Thicknesses are presented as mean ± std.

Material	Extractable from mould	Watertight	Wall thickness (mm)
Superflex (3DMS)	N/A	y	0.549 ± 0.017
RT 601	n	n	N/A
HT 33	y	n	0.313 ± 0.228
Vascuflex (3DMS)	N/A	y	0.930 ± 0.281

5.4 Surrounding tissue materials

Maximum diameter of beads was measured to be 9.2 ± 0.5 mm. The measured relation between diameter and water content is in most cases lower than the expected relation, as is visible in Figure 5-5. The average deviation between the three measured samples per condition was at most 3.2 %.

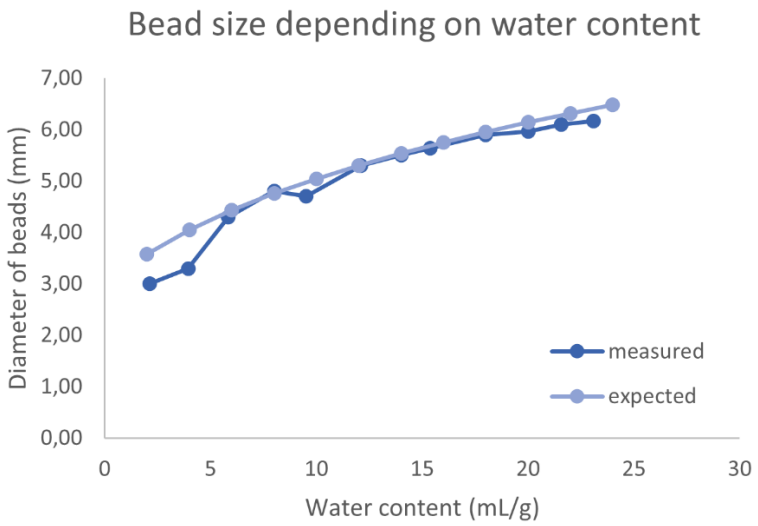

Figure 5-5: Graph of the expected bead size function as well as the means of measured bead sizes. Each dot represents one of the beads-to-water ratios that was included in the experiment.

The maximum movement of the vein on inserting an insertion device is shown in Table 5-3. Under all three devices, the vein movement was limited with beads as surrounding tissue compared to no surrounding tissue (air).

Table 5-3: Movement of the apex of the U-shaped vein on insertion of various devices. Air refers to the condition with no surrounding material. Beads refer to the condition where beads are used as surrounding material.

Insertion device	Air	Beads
4 Fr catheter	0.09 mm	0.03 mm
8 Fr Cannula	0.46 mm	0.33 mm
Metal guide wire	0.61 mm	0.31 mm

5.5 Survey testing

The resulting setup for use in survey testing is shown in Figure 5-6A.

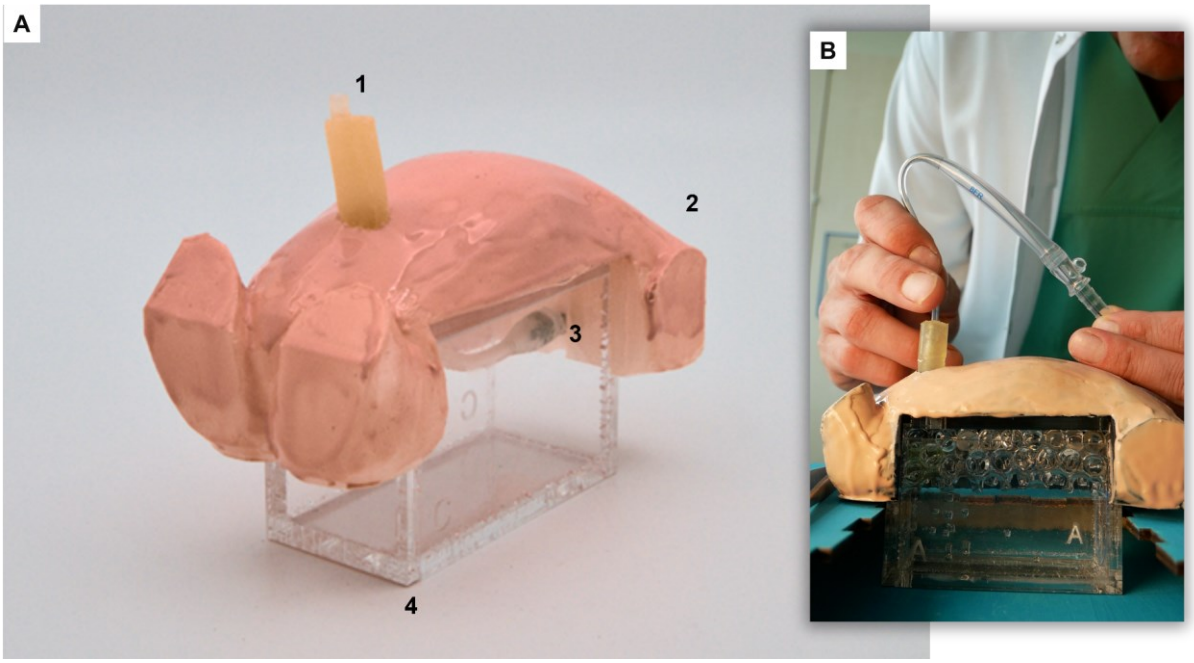

Figure 5-6: Setup used in survey testing. **A:** Setup C, **1** Umbilical structure consisting of Wharton jelly and vein, **2** outer shell, **3** Connection point of the umbilical vein, **4** PMMA box, **B:** Cannulating the umbilical vein using an 8 Fr cannula by a neonatologist.

5.5.1 Demographic

A total of 5 men and 6 women filled out the entire questionnaire. All participants were either neonatologists or paediatricians. Most had performed around a hundred umbilical cord catheterizations. The main purpose of these umbilical catheterizations was either providing nutrition or medication for which a 4 Fr was used in most cases. One participant had had physical synthetic training experience, others either had none or pure theoretic training. A complete elaboration of the survey results is presented in Annex D.

5.5.2 Umbilical cord

In terms of compliancy, the artificial vein made of silicone (HT 33) was consistently ranked next to the Real UV. In terms of roughness, silicone came closest to the Real UV most often, though not in all cases, see Table 5-4.

Table 5-4: Distance to the ranking position of the sample with respect to the Real UV. Data is represented as first quartile, median, and third quartile. Maximum distance is three, minimum distance is one.

Sample	Compliancy			Roughness		
	Q1	median	Q3	Q1	median	Q3
Vascuflex	2	3	3	1	2	2,5
Superflex	2	2	2.5	1.5	2	3
Silicone	1	1	1	1	1	2

Participants consistently recommended that Wharton's jelly should become less stiff and more compliant. Similarly, the recommendation was to not increase roughness, but to make it more slippery. The aggregated score for more compliancy was 1.36 and for more slippery was 1.18. Likert scale responses are represented in a stacked bar chart in Figure 5-7.

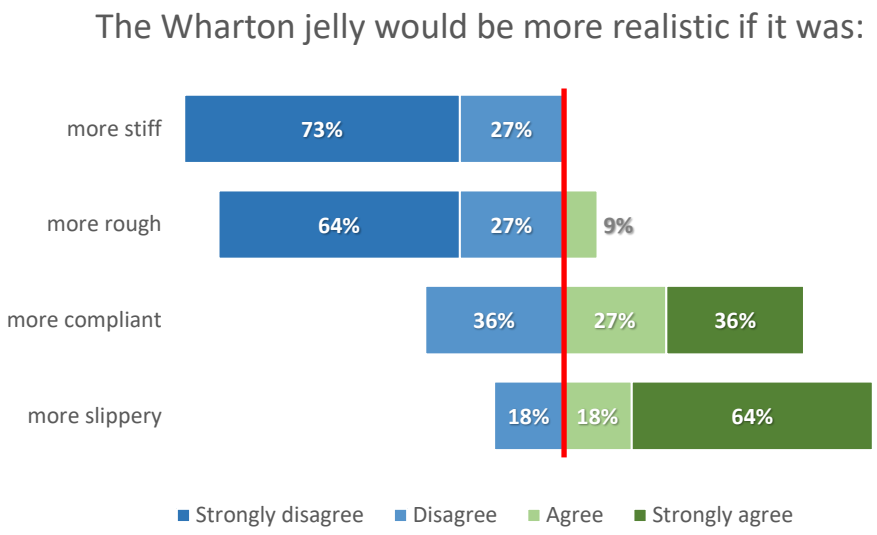

Figure 5-7: Results of the Likert scale question regarding improvement in realism of the Wharton's jelly. The red line represents the neutral line. Blue sections sum up to 100 % bar rounding errors.

5.5.3 Cannulation procedure

Ranking of materials with respect to roughness gave results with variances between 1.7 and 4.4 for a total of 7 ranks, for boxplots see Figure 5-8.

To show the difference in ranking, both the relative as well as combined absolute differences are shown in Table 5-5. Negative relative positions are perceived to have less resistance than Real UV. This is the case for all setups except Setup B (Superflex). However, this is in stark contrast to its counterpart, Setup C, where the difference in mean position is larger than observed among the other setups.

The question regarding movement of the vein (Q20), was left out of the survey due to imperceptibility. In the words of one participant: "That you can hardly feel in the human body.".

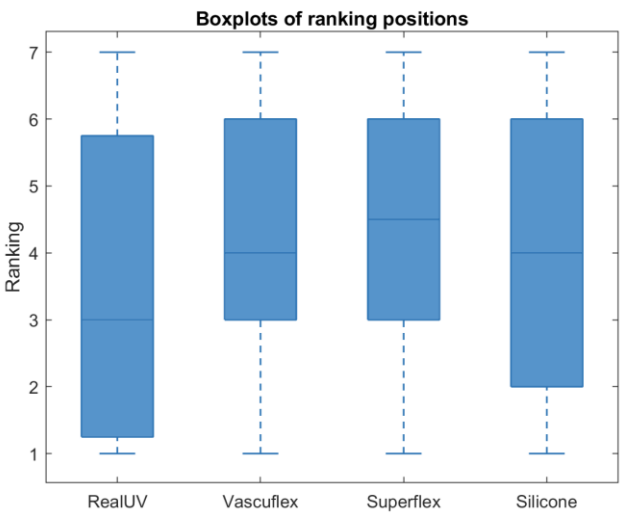

Figure 5-8: Box and whisker plots showing the spread of the different positions the materials were ranked as. Whiskers are according to Tukey's method.

Table 5-5: Distance to HUV in ranking for each setup. Setups are indicated by a random alphabetical letter. Data is represented as first quartile, median, and third quartile. Maximum distance is 5, minimum distance is 1. Negative relative ranking positions are perceived to have less resistance than Real UV.

Sample	Material	Relative ranking position difference			Absolute ranking position difference		
		Q1	median	Q3	Q1	median	Q3
Setup A	Vascuflex	−2.5	−1	1	1	2	2.75
Setup E		−2	−2	−1			
Setup B	Superflex	−2.5	1	3	1	2.5	4
Setup C		−3.5	−1	1			
Setup D	Silicone	−4.5	−1	3	2.25	3	5
Setup F		−3	−1	2.5			

5.5.4 Puncturing and tearing behaviour

Recommendations with regard to puncturing and tearing behaviour are presented in Figure 5-9. Aggregated scores for “easier to puncture” and “easier to tear” are presented in Table 5-6.

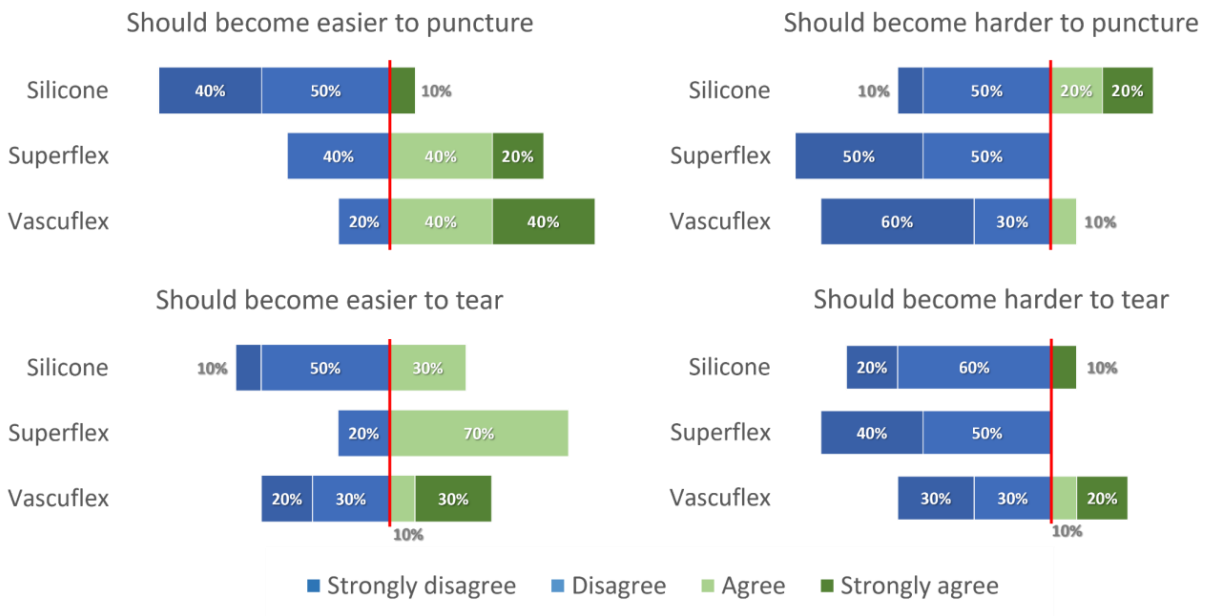

Figure 5-9: Results from the Likert scale questions regarding puncturing and tearing. Blue sections sum up to 100 % bar rounding errors. Left of the red line corresponds to negative responses, to the right corresponds to positive responses.

Table 5-6: Median score for tearing and puncturing. Disagreement scores negative points, agreement scores positive points. A score closer to zero means change is less urgent. Data is represented as first quartile, median, and third quartile.

Sample	Should become easier to tear			Should become easier to puncture		
	Q1	median	Q3	Q1	median	Q3
Vascuflex	−1.5	0	3	2	2.5	4
Superflex	0.5	2	3	0	2.5	3
Silicone	0	0	1.5	−2.75	−0.5	0

6 Discussion

This research aimed to identify materials and production methods suitable for creating the venous tract of a neonate, as part of an umbilical cannulation simulator. Mechanical properties of human umbilical veins, as found in literature, were used to select materials for use in a physical model. These models were then used to validate the materials in a real-world setting. First, the results of the mechanical testing will be discussed individually, then these will be related to the results from the survey test.

Hamedani et al. [33] showed that the umbilical veins behave anisotropically with respect to their longitudinal and circumferential directions. The silicones included in this study are not known to exhibit anisotropic behaviour [40]. The 3D-printable materials, however, might exhibit anisotropic behaviour, though no significant differences between the horizontal and vertical directions were found ($p > 0.05$).

Both the silicones and the HUV do show non-linear behaviour, as is clear from Figure 5-1. Thus, comparing these through single-value properties, such as Young's modulus, does not capture the full story. The tangent modulus differs greatly depending on strain range in case of HUV, as is visible from Figure 5-2A,B. The value for tangent modulus in the linear portion of the graph, which corresponds to Young's modulus, is four times the value of the tangent modulus in the first 10 % strain. In comparing these non-linear materials, multiple different parameters should thus be taken into account and applied when relevant.

The most compliant materials, HT 33 (silicone) and Superflex, were ranked closer to HUV than Vascuflex, the least compliant material, as shown in Table 5-4. Combining this with both tangent moduli presented in Figure 5-2, it seems that the first 10 % strain (Figure 5-2B) would be a better predictor for realistic haptic feedback. If Young's modulus were the better predictor, Vascuflex would have been rated better since its Young's modulus is closer to E_{HUV}. Thus, if a comparison regarding handling needs to be made, comparing tangent moduli based on a low strain range (up to 10 %) should be considered.

Not only do the values for tangent modulus change depending on the portion of the strain range, but different ways of calculating specifically Young's modulus are also inconsistent, as is visible from Table 5-1. Most notably in the case of RT601, where the Young's modulus as derived from the Shore A hardness is almost 1.7 times the Young's modulus as derived from the linear portion of the graph. Although Shore A is easier to measure, its Young's modulus is derived from a modelled mechanical contact response [19] and thus not necessarily equal to the definition of Young's modulus. Therefore, when available, the linear portion of the graph is the preferred method for determining Young's modulus.

The materials HT 33 (silicone), Vascuflex, and Superflex were used in simulators in order to carry out survey testing.

The survey results indicated that the silicone model was better in terms of flexibility as well as puncturing and tearing behaviour, as presented in Table 5-4 and Table 5-6 respectively. All participants consistently recommended that the Wharton's jelly should be more compliant, see Figure 5-7. Currently, it is too stiff and stays upright, as is visible in Figure 5-6.

Although the silicone model can be considered the most realistic based on the results of the survey test, producing water-tight models with even wall thicknesses out of silicone was found to be problematic. This is especially the case for models with higher complexity, for example, when bifurcations were introduced. Due to the different directions, gravity affected the material differently. This caused increased wall-thickness in positively sloped portions and decreased wall-thickness in negatively sloped portions. These thin portions would easily tear during extraction from the mould. Rotating the mould during curing could be considered to even out the effect of gravity and would thus presumably even out wall-thickness as well.

Going up even further in complexity, such as including multiple bifurcations and heart chambers, 3D printing becomes the preferred option. Coating moulds with this many features would require complex rotations to prevent uneven wall thicknesses. Alternatively, if wall-thickness is to be controlled using inner moulds, careful consideration should be taken to how they are kept in place. Extracting inner moulds also becomes increasingly difficult with higher complexity. 3D printing allows for more flexibility in terms of complexity. In future research, similar tactics to Garcia et al. [41] could be incorporated to finetune 3D-printable materials. The material they used, along some recently available 3D-printable silicones, is available in Annex H.

Comparing the ultimate tensile strength (Figure 5-2C) to the results of the survey test, no clear relation can be discovered. The tensile test (Figure 5-2C) resulted in a mean UTS of 0.8 MPa for Vascuflex, 0.5 MPa for Superflex, and 5.8 MPa for HT 33. The UTS of HUV was found to be 1.7 MPa. According to the survey both Vascuflex and HT 33 should not become easier to tear (Table 5-6). Because Vascuflex has a lower UTS while HT 33 has a higher UTS than HUV, no clear correlation can be drawn between UTS and tearing.

Both Vascuflex and Superflex have a lower UTS than HUV. Both should become easier to puncture. HT 33 has a higher UTS and should not become easier to puncture. Thus, there is a tendency that a material with a low UTS should become easier to puncture, while a high UTS should become harder to puncture. However, this does seem illogical. "Easier to puncture" might have been differently interpreted than in terms of strength.

No clear relation can be discovered between the breaking strain (Figure 5-2D) and the scores for tearing and puncturing (Table 5-6) either. Both a high breaking strain (HT 33, 440 %) and a breaking strain similar to HUV (Vascuflex, 33 %) get a score of 0 for becoming easier to tear. There is a tendency that a material with a breaking strain higher than HUV should become harder to puncture, while a material with a comparable strain to HUV should not become harder to puncture.

6.1 Limitations and impact

Mechanical testing was limited to static mechanical behaviour only. Dynamic behaviour might be a relevant factor in handling the umbilical vein. For example, during the survey testing, closing of

the vessel after opening was mentioned as a relevant behaviour for realism. Dynamical properties, such as stress relaxation and creep, could be used to understand and compare this behaviour to synthetic materials. Some work regarding viscoelastic evaluation of the HUV has already been performed by Dongyuan Li et al. [42]. However, the closing of the vessel is likely to be an emergent behaviour, depending on both the umbilical vein as well as the surrounding Wharton's jelly. These would both need to be taken into account simultaneously. During this research, both have been developed separately. Insertion of the cannula will induce a dynamic response from the material, which is currently not accounted for. This could lead to unrealistic behaviour in those settings. However, for cannula development, matching static behaviour should suffice for static testing.

Regarding the survey, most participants reported working with a smaller than 4 Fr catheter when catheterizing umbilical veins. Only two out of eleven participants had performed cannulation with a cannula of similar size to that intended to be used with the simulator (10 Fr), albeit on piglet umbilical cords. Still, this should not invalidate those participants, as all participants were highly experienced in handling human umbilical cords. The size difference is, however, a notable limitation regarding cannula development. A 10 Fr cannula has more resistance with the wall than a small diameter catheter. The effect this has on realistic haptics has not been extensively tested. In future research, changes in realism as a result of cannula size should be included.

In analysing the results of the question regarding resistance of the vein (Q20), the wide-ranging variance in terms of ranking (Figure 5-8) could be attributed to different interpretations of the question. Some interpreted resistance as the continuous resistance due to wall friction, while some interpreted it as obstruction within the vein or constriction as a result of pressure from the Wharton's jelly. Including clearly phrased questions for both interpretations should decrease variance in the answers.

The question regarding the movement of the vein (Q22) was omitted from the questionnaire because it was impossible to evaluate. Participants reported that vein movement within the body is imperceptible via insertion of a catheter. Movement of the vein, however, could prove important in the development of a cannula, i.e. for determining the maximum allowed stiffness. According to test results presented in Table 5-3, movement of the vein is extremely limited on insertion of various devices, even when no surrounding material is present. An alternative way of validating this with vein movement in vivo should still be considered. Additionally, alternative materials for surrounding tissue can be considered. Only Konnyaku Jelly, water beads, and Carbopol were currently taken into account and their evaluation as presented in chapter 4.4 is subjective. Future simulators could be more anatomically inspired, such as by mimicking the intestines. This might prove useful to, for example, test the bend radius of the cannula during development.

Simulators used during the survey testing were limited in several ways. A hard plastic, 3D printed torso was used, which decreases the simulator in terms of fidelity. In future simulators, soft materials should be considered to better represent the torso in terms of compliancy. This is, however, not a priority for cannula development.

Secondly, the anisotropic differences present in the human umbilical vein were not represented in the simulators. This could thus also not be validated. Values for longitudinal direction were used for comparing mechanical properties. The circumferential mechanical properties of HUV might, however, influence circumferential properties of the cannula as well.

Thirdly, testing the compliancy within the survey was affected by varying wall thicknesses. Both between materials, but also within materials. As is visible in Table 5-2, both HT 33 and Vascuflex

exhibit high variability in terms of wall thickness. Nevertheless, in terms of creating a realistic simulator, this variability would be of little consequence, real human umbilical veins similarly exhibit high variability in wall thickness [16].

Finally, only the umbilical vein was included in the simulator in order to feasibly construct six simulators. In future simulators, the venous tract as presented in Figure 5-3 should be incorporated. The model as presented in Figure 5-3, however, is still limited in terms of accuracy. The venous tract, apart from the umbilical vein, consists of a downscaled adult model. Proportions of the adult model were matched by hand, and only in terms of the length of the inferior vena cava. Additionally, the connection point between the umbilical vein and inferior vena cava was based on position and angle only. Connection to the portal veins was omitted. Use of either CT or MRI scans of preterm neonates would be ideal but are challenging to acquire.

7 Summary and Outlook

Both direct 3D printing and silicone coating techniques show potential for the production of a realistic umbilical cannulation simulator. However, silicone coating techniques are limited to simple models such as single veins only. Furthermore, coating is also limited in terms of controlling the thickness.

For larger, more complex anatomically correct models, direct 3D printing is preferred to ensure more control over wall thickness. Even at the expense of matching mechanical properties. Although Vascuflex has better matching material properties, Superflex was found to be better performing when incorporated in a simulator, according to the survey.

Moulding techniques that required the removal of an inner mould were not found to be successful.

The flexibility of the umbilical cord is an important factor in creating a realistic anatomically correct cannulation simulator. The molten gummy bears were found to be too stiff to represent Wharton's jelly realistically, especially when handling. The stiffness of the vein should not be linear and should be low for the first 10 % of the strain range, with a tangent modulus of around 1 MPa. No evidence was found for UTS and breaking strain to be of relevance in the realism of puncturing and tearing.

Taking into account stress relaxation and creep can help explain other factors that increase realism, such as the closing of vessels after opening.

8 Terms and Abbreviations

8.1 Terms

Anastomosis
The place where two blood vessels connect [43]

Wharton's Jelly
Gelatinous substance which makes up the umbilical cord

Cannula
A thin tube that can be put into the body, for example to put in medicine or remove blood [43], *in this thesis used to indicate transport of larger volumes*

Catheter
A long, very thin tube used to take liquids out of the body [43], *in this thesis used to indicate transport of smaller volumes*

8.2 Abbreviations

DC *Ductus venosus*

DLP *Digital Light Processing*

E *Young's modulus*

ECMO *Extracorporeal Membrane Oxygenation*

ECPR *Extracorporeal Cardiopulmonary Resuscitation*

FDM *Fused Deposition Modelling*

Fr *French gauge, measurement of catheter size. 1 Fr = 1/3mm*

GA *Gestational age*

RDS *Respiratory Distress Syndrome*

SBME *Simulation Based Medical Education*

SLA *Stereolithography*

UC *Umbilical Cord*

UTS *Ultimate Tensile Strength*

UV *Umbilical Vein*

VC *Vena Cava*

9 List of Figures

Figures from Annex

10 List of Tables

Tables from Annex

11 References

[1] H. Usuda *et al.*, "Artificial placenta technology: History, potential and perception," *Placenta,* vol. 141, pp. 10-17, Sep 26 2023, doi: 10.1016/j.placenta.2022.10.003.

[2] C. M. Burgos, B. Frenckner, and L. M. Broman, "Premature and Extracorporeal Life Support: Is it Time? A Systematic Review," *Asaio J,* Sep 28 2021, doi: 10.1097/MAT.0000000000001555.

[3] D. Warburton, "Overview of Lung Development in the Newborn Human," *Neonatology,* vol. 111, no. 4, pp. 398-401, 2017, doi: 10.1159/000458465.

[4] S. Rosenblum, A. Pal, and K. Reidy, "Renal development in the fetus and premature infant," *Semin Fetal Neonatal Med,* vol. 22, no. 2, pp. 58-66, Apr 2017, doi: 10.1016/j.siny.2017.01.001.

[5] J. E. Brumbaugh *et al.*, "Outcomes of Extremely Preterm Infants With Birth Weight Less Than 400 g," *JAMA Pediatrics,* vol. 173, no. 5, pp. 434-445, 2019, doi: 10.1001/jamapediatrics.2019.0180.

[6] "Artificial Placenta (ArtPlac) - Miniaturized Integrated Lung and Kidney Support for Critically Ill Newborns," ed, 2022.

[7] G. C. Lewis, S. A. Crapo, and J. G. Williams, "Critical skills and procedures in emergency medicine: vascular access skills and procedures," *Emerg Med Clin North Am,* vol. 31, no. 1, pp. 59-86, Feb 2013, doi: 10.1016/j.emc.2012.09.006.

[8] T. Sawyer, M. Gray, M. Hendrickson, E. Jacobson, and R. Umoren, "A Real Human Umbilical Cord Simulator Model for Emergency Umbilical Venous Catheter Placement Training," *Cureus,* vol. 10, no. 11, p. e3544, Nov 5 2018, doi: 10.7759/cureus.3544.

[9] D. A. Ghazali, Q. Cholet, C. Breque, and D. Oriot, "Development and Testing of a Hybrid Simulator for Emergent Umbilical Vein Catheter Insertion Simulation Training," *Simul Healthc,* vol. 18, no. 5, pp. 333-340, Oct 1 2023, doi: 10.1097/SIH.0000000000000700.

[10] A. Mahmoud, A. Alsalemi, F. Bensaali, A. A. Hssain, and I. Hassan, "A Review of Human Circulatory System Simulation: Bridging the Gap between Engineering and Medicine," *Membranes (Basel),* vol. 11, no. 10, Sep 28 2021, doi: 10.3390/membranes11100744.

[11] J. L. Thompson *et al.*, "Construction of a Reusable, High-Fidelity Model to Enhance Extracorporeal Membrane Oxygenation Training Through Simulation," *Advances in Neonatal Care,* vol. 14, no. 2, 2014, doi: 10.1097/ANC.0000000000000054.

[12] G. C. Schoenwolf, S. B. Bleyl, P. R. Brauer, P. H. Francis-West, and W. J. Larsen, *Larsen's Human embryology*, Sixth edition ed. Philadelphia: Elsevier Philadelphia (in eng), 2021.

[13] P. D. T. W. Sadler, *Langman's Medical Embryology*, 12th Edition ed. 2012.

[14] E. Mavrides, G. Moscoso, J. S. Carvalho, S. Campbell, and B. Thilaganathan, "The anatomy of the umbilical, portal and hepatic venous systems in the human fetus at 14–19 weeks of gestation," *Ultrasound in Obstetrics & Gynecology,* vol. 18, no. 6, pp. 598-604, 2001, doi: 10.1046/j.0960-7692.2001.00581.x.

[15] N. Rochow *et al.*, "Artificial placenta--lung assist devices for term and preterm newborns with respiratory failure," *Int J Artif Organs,* vol. 36, no. 6, pp. 377-91, Jun 25 2013, doi: 10.5301/ijao.5000195.

[16] R. Gayatri *et al.*, "Structural Analysis of the Umbilical Cord and Its Vessels in Intrauterine Growth Restriction and Pre-eclampsia," *Journal of Fetal Medicine,* vol. 04, no. 02, pp. 85-92, 2023, doi: 10.1007/s40556-017-0118-2.

[17] M. R. Thomas, J. K. Bhatia, S. Kumar, and D. Boruah, "The histology and histomorphometry of umbilical cord cross section in preeclampsia and normal pregnancies: a comparative study," *Journal of Histotechnology,* vol. 43, no. 3, pp. 109-117, 2020/07/02 2020, doi: 10.1080/01478885.2020.1734741.

[18] A. Jarosz-Lesz, K. Michalik, and I. Maruniak-Chudek, "Baseline Diameters of Inferior Vena Cava and Abdominal Aorta Measured by Ultrasonography in Healthy Term Neonates During Early Neonatal Adaptation Period," *Journal of Ultrasound in Medicine,* vol. 37, no. 1, pp. 181-189, 2018/01/01 2018, doi: 10.1002/jum.14324.

[19] B. J. Briscoe and K. S. Sebastian, "An Analysis of the "Durometer" Indentation," *Rubber Chemistry and Technology,* vol. 66, no. 5, pp. 827-836, 1993, doi: 10.5254/1.3538347.

[20] *ISO 48-4 Rubber, vulcanized or thermoplastic — Determination of hardness* — I. O. f. Standardization, Geneva, 2018.

[21] J. O. Lopreiato and T. Sawyer, "Simulation-Based Medical Education in Pediatrics," *Academic Pediatrics,* vol. 15, no. 2, pp. 134-142, 2015/03/01/ 2015, doi: 10.1016/j.acap.2014.10.010.

[22] H. Blencowe *et al.*, "Born Too Soon: The global epidemiology of 15 million preterm births," *Reprod Health,* vol. 10, no. 1, p. S2, 2013/11/15 2013, doi: 10.1186/1742-4755-10-S1-S2.

[23] M. Delnord and J. Zeitlin, "Epidemiology of late preterm and early term births – An international perspective," *Seminars in Fetal and Neonatal Medicine,* vol. 24, no. 1, pp. 3-10, 2019/02/01/ 2019, doi: 10.1016/j.siny.2018.09.001.

[24] T. Sawyer, K. Hara, M. W. Thompson, D. S. Chan, and B. Berg, "Modification of the Laerdal SimBaby to Include an Integrated Umbilical Cannulation Task Trainer," *Simulation in Healthcare,* vol. 4, no. 3, pp. 174-178, 2009, doi: 10.1097/SIH.0b013e31817bcaeb.

[25] "Premature Anne™ | Products & Pricing (laerdal.com) " https://laerdal.com/us/item/290-00050 (accessed 18-06, 2024).

[26] "Build Confidence in Handling Pre-Term Births." https://laerdal.com/us/PrematureAnne (accessed 18-06, 2024).

[27] M. Jiménez, L. Romero, I. A. Domínguez, M. d. M. Espinosa, and M. Domínguez, "Additive Manufacturing Technologies: An Overview about 3D Printing Methods and Future Prospects," *Complexity,* vol. 2019, 2019/02/19 2019, doi: 10.1155/2019/9656938.

[28] "How to dissolve Ultimaker PVA." https://support.makerbot.com/s/article/1667410781980 (accessed 29-02, 2024).

[29] "Formlabs 3L." https://formlabs.com/3d-printers/form-3l/ (accessed 03-03-24, 2024).

[30] "Elastic 50A Resin V2 Datasheet," in *Resin for Soft Flexible Parts*, ed: Formlabs.

[31] "IMPROVE YOUR WORKFLOW WITH SILICONE 3D PRINTING," ed: Lynxter, 2023.

[32] "S180 Silicone 3D Printer." https://www.sandraw.com/product-page/s180-silicone-3d-printer (accessed 13-06-2024, 2024).

[33] B. A. Hamedani, M. Navidbakhsh, and H. A. Tafti, "Comparison between mechanical properties of human saphenous vein and umbilical vein," *Biomed Eng Online,* vol. 11, no. 1, p. 59, 2012/08/23 2012, doi: 10.1186/1475-925X-11-59.

[34] "Lynxter, CUSTOMIZED PRODUCTION LIMITLESS MATERIALS." https://lynxter.fr/en/ (accessed 06-06-2024, 2024).

[35] "Sandraw." https://www.sandraw.com/ (accessed 06-06-2024, 2024).

[36] *Rubber, vulcanized or thermoplastic — Determination of tensile stress-strain properties*, I. O. f. Standardization, Geneva, 2017.

[37] S. Lochem, "Developing a realistic venous model for in-vitro application of the eduECMO trainer," EOST, University of Twente, 2023.

[38] M. Tanigawa, T. Chu, R. E. Lewiss, and A. Au, "Konnyaku jelly: A quick preparation and cost effective ultrasound-guided IV phantom model," *The Journal of Vascular Access,* vol. 24, no. 2, pp. 271-276, 2023/03/01 2021, doi: 10.1177/11297298211030814.

[39] "Carbopol® ETD 2020 polymer." https://www.lubrizol.com/Personal-Care/Products/Product-Finder/Products-Data/Carbopol-ETD-2020-polymer (accessed 07-06-2024, 2024).

[40] R. H. W. Lam and W. Chen, *Biomedical Devices: Materials, Design, and Manufacturing*. Springer International Publishing, 2019.

[41] J. Garcia, M. AlOmran, A. Emmott, R. Mongrain, K. Lachapelle, and R. Leask, "Tunable 3D printed multi-material composites to enhance tissue fidelity for surgical simulation," *Journal of Surgical Simulation,* vol. 5, no. 1, pp. 87-98, 2018, doi: 10.1102/2051-7726.2018.0013.

[42] D. Li, D. Xu, P. Li, J. Wei, K. Yang, and C. Zhao, "Viscoelastic evaluation of fetal umbilical vein for reconstruction of middle cerebral artery," *Neural Regen Res,* vol. 8, no. 32, pp. 3055-62, Nov 15 2013, doi: 10.3969/j.issn.1673-5374.2013.32.009.

[43] "Cambridge dictionary of English," ed, 2024.

12 Annex

Declaration use of AI

During the writing of this thesis, tools such as ChatGPT and Google Gemini were used as inspiration for improving sentence structure and wording.

The author bears full responsibility for the content of the work written in this thesis.

Annex A Creating Veins

A.1 Coating

As wall thicknesses of less than 1 mm need to be recreated, coating the inner wall of a tubular shape was experimented with. A mould was created such that the outer diameter of the resulting vessel was 7.8 mm, illustrated in Figure Annex A.1-1A. Moulds were printed using an Ultimaker 3 (Ultimaker B.V., Geldermalsen) using PLA. Elastosil RT 625 (Wacker Chemie AG, Munich) was mixed in ratio according to the TDS using a Wamix Touch (Wassermann, Hamburg). This was then poured into the funnel and left until cured.

The process was repeated with HT 33 (Zhermack SpA, Badia Polesine).

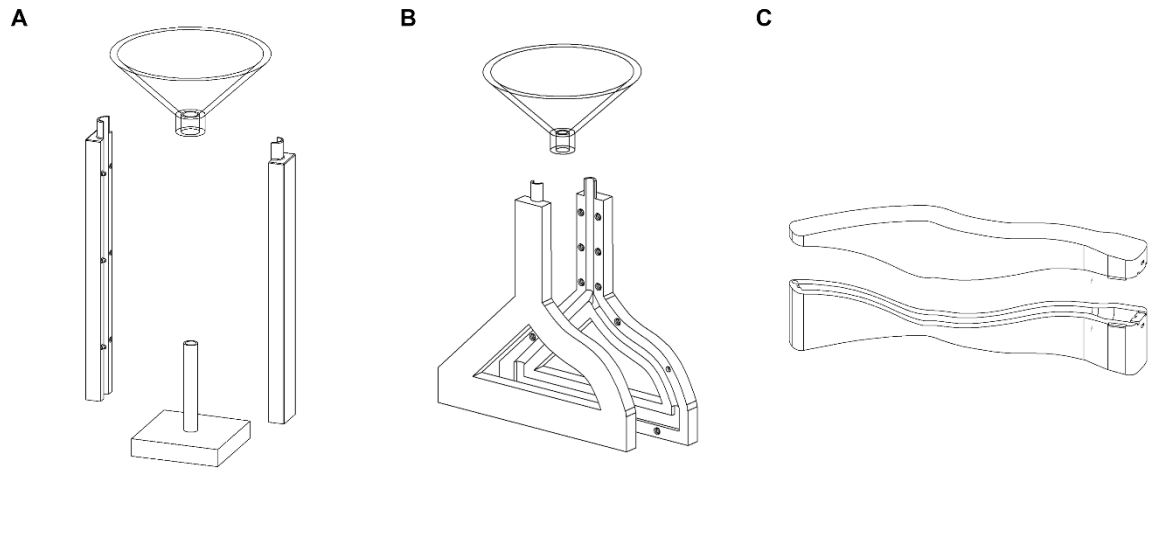

Figure Annex A.1-1: **A:** Mould for testing coating of the inner wall. **B:** Mould for testing coating in case of different. **C:** Mould used for creating survey setups.

To test the same principle on increased model complexity, a mould for a bifurcated vein was created, illustrated in Figure Annex A.1-1B.

The mould used for creating anatomically accurate umbilical veins is presented in Figure Annex A.1-1C.

A.2 Moulding

A mould containing an inner mould was considered for more control over wall thicknesses. Outer moulds and inner moulds, Figure Annex A.2-1, were printed using a Bambu Lab X1-Carbon (Bambu Lab, Austin) using PLA. Different materials for inner mould were considered as well: a nylon mould was printed using a FORMIGA P101 (EOS GmbH - Electro Optical Systems, Krailing) SLS printer. While a Grey Resin mould was printed using a Formlabs Form 3L (Formlabs, Somerville). After curing, the inner moulds were attempted to be separated from the silicone product.

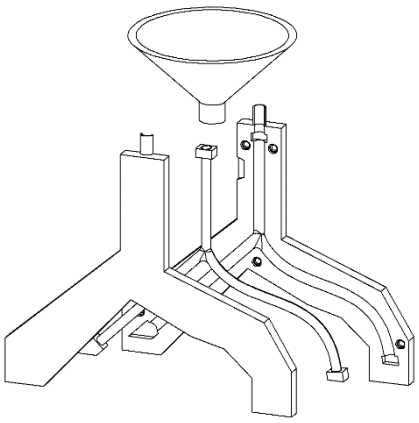

Figure Annex A.2-1: Bifurcated vein mould, including inner mould.

A.3 3D printing

Anatomically accurate veins were 3D printed at 3DMS in both their Vascuflex and Superflex materials. STL provided for printing is shown in Figure Annex A.3-1

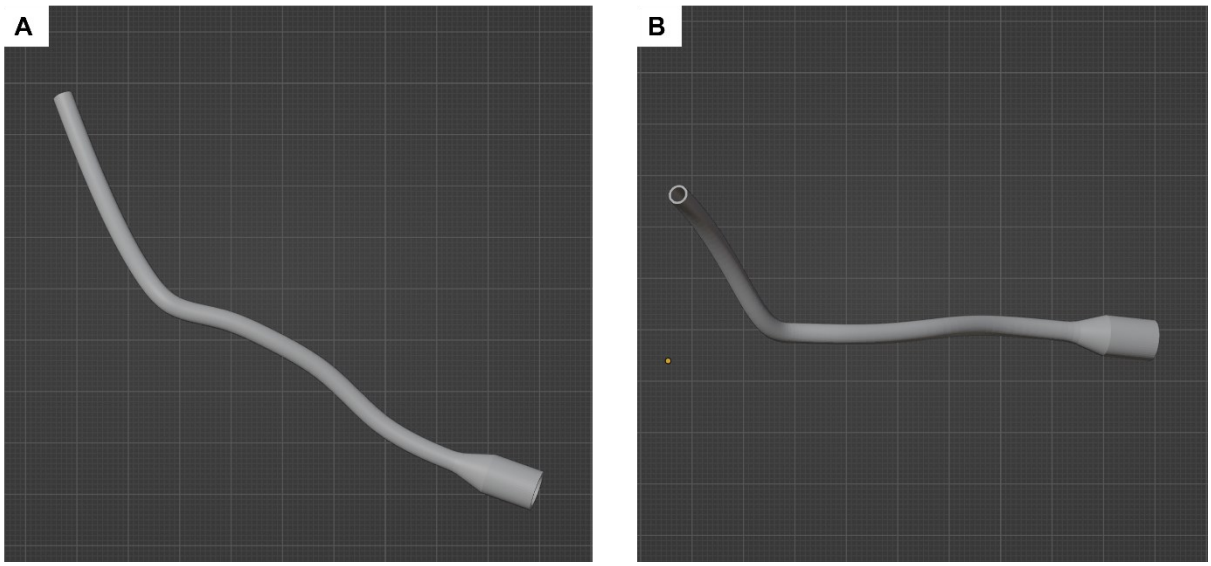

Figure Annex A.3-1: STL file provided for printing to 3DMS. A: Lateral view. B: Frontal view.

Annex B Creating survey setups

This document describes the creation of the body setups used in survey testing. It consists of three distinct parts:

- The phantom torso
- The inner body enclosure
- The umbilical structure

B.1 The phantom body

For the creation of 1 phantom body:

- 3D printed torso [EOST - 05_VanDerWoerd_LWd\08_Production\External_body\baby_torso_flipped.STL]
- HT 33 or similar two-component silicone
- Flesh silicone coloring
- Paint brush

Steps

1. Print the torso in PLA. In our case an Ultimaker 5S (Ultimaker B.V., Geldermalsen) was used.
2. Measure 10 grams of HT 33 base, as well as 10 grams of HT 33 catalyst.
3. Add 1.5 % flesh silicone coloring.
4. Mix using a Wamix Touch (Wassermann, Hamburg).
5. Coat the torso in 4 layers of silicone using a paint brush.

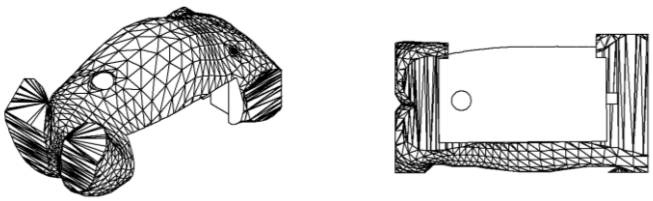

Figure Annex B.1-1: STL file of the torso

B.2 Inner body enclosure

For the creation of 1 inner body enclosure:

- Clear PMMA sheet, thickness 5 mm, 237 x 102 mm
- Acrifix
- Laser-cut file [EOST - 05_VanDerWoerd_LWd\09_Validation\Material_Survey\test_setup\box\single_box.ai]

Steps

1. The PMMA can be cut using a Trotec Speedy 300 (Trotec Laser GmbH, Marchtrenk Austria).
2. Assemble the box from top to bottom. Do not connect the top part. This can slide in later.

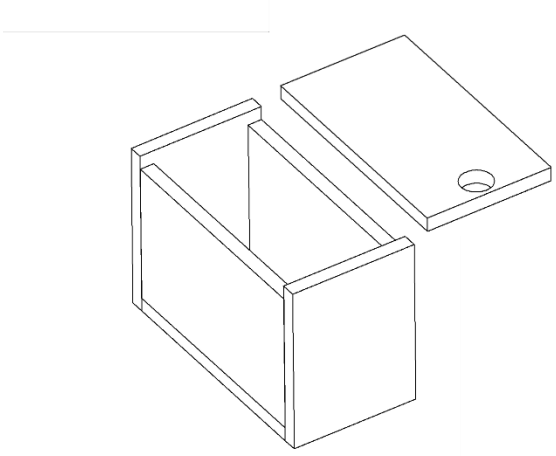

Figure Annex B.2-1: Box for containment of the vein and surrounding material

B.3 Umbilical structure

For the creation of 1 silicone umbilical structure:

- HT 33, RT 625 or other two-component silicone
- 3D printed mould, consisting of
  - [EOST - 05_VanDerWoerd_LWd\08_Production\UmbilicalVein\UV_model\mould\bottom.STL]
  - [EOST - 05_VanDerWoerd_LWd\08_Production\UmbilicalVein\UV_model\mould\top.STL]
- Clamps
- Paint brush
- Silicone compound
- 5 x 5 mm neodymium magnets
- 5 grams of Gummy Bears
- Hot plate
- Beaker
- Water
- ½" Silicone tubing
- Clay
- Cornstarch

Steps Silicone Veins

1. Print the bottom and top part of the mould in PLA. In our case a Bambu Lab X1C (Bambu Lab, Austin) was used.
2. Mix 10 grams of silicone in their respective weight ratio using a Wamix Touch (Wassermann, Hamburg).
3. Coat the inside of both parts of the mould using a brush.
4. Clamp the two sides together, position lengthwise and wait until silicone is cured.
5. Once cured, open the mould and glue a neodymium magnet into the proximal side using silicone compound.

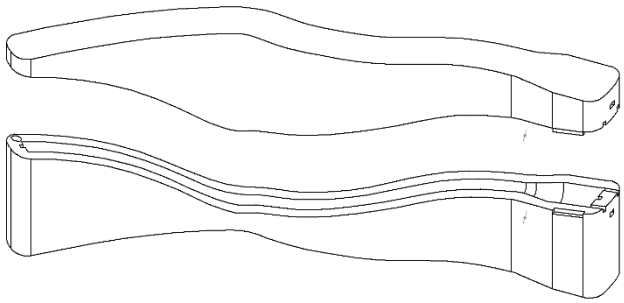

Figure Annex B.3-1: Two-part mould for creating the umbilical vein. The proximal part is at the right, the distal part to the left.

Steps Wharton Jelly

1. Cut the ½" Silicone tubing to desired length, appx. 5cm.
2. Put the vein into the tubing while plugging the bottom using clay.
3. Add 5 grams of gummy bears together with 1 ml water to a beaker.
4. Heat on the hot plate to 120 °C, or until molten. Alternatively the *au bain marie* method can be used.
5. Pour the molten gummy bears into the silicone tubing.
6. Let solidify overnight in a fridge.
7. Cut open the silicone tubing along its length.
8. Roll the umbilical cord through corn starch.

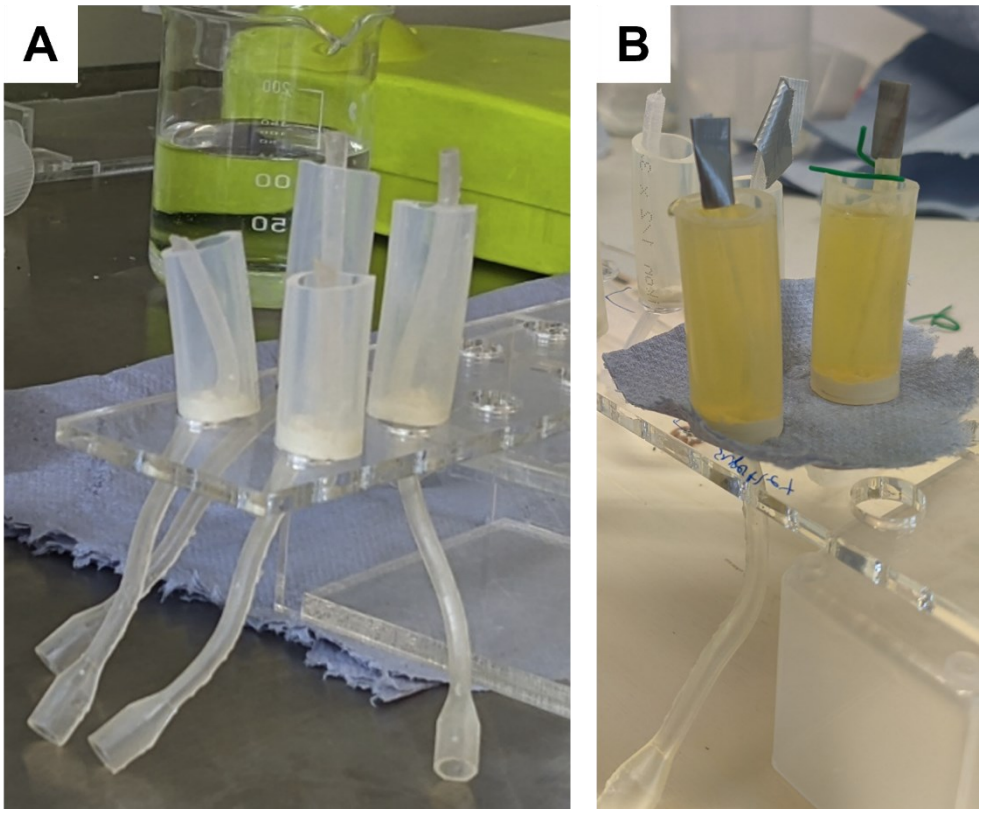

Figure Annex B.3-1: Creating umbilical cords. **A**: the vein in the tube, bottom plugged with clay. **B**: the tubing filled with gelatine.

B.4 Complete construction

The following additional materials are needed to complete construction

- Completed parts B.1, B.2 and B.3
- 5x5mm neodymium magnet
- 2 grams of water beads
- 140ml water

Steps

1. Put 2 grams into the box and add 140 ml of water, or until full.
2. Let soak until full bead-size is reached.
3. Pull the umbilical cord through the torso and the top part of the box. Tweezers can be used to pull the Wharton jelly into the umbilical opening of the torso.
4. Connect a magnet on the outside of the box with the magnet of the vein. This way the vein be positioned to liking. The magnet on the outside can slide into the torso using the provide slit.

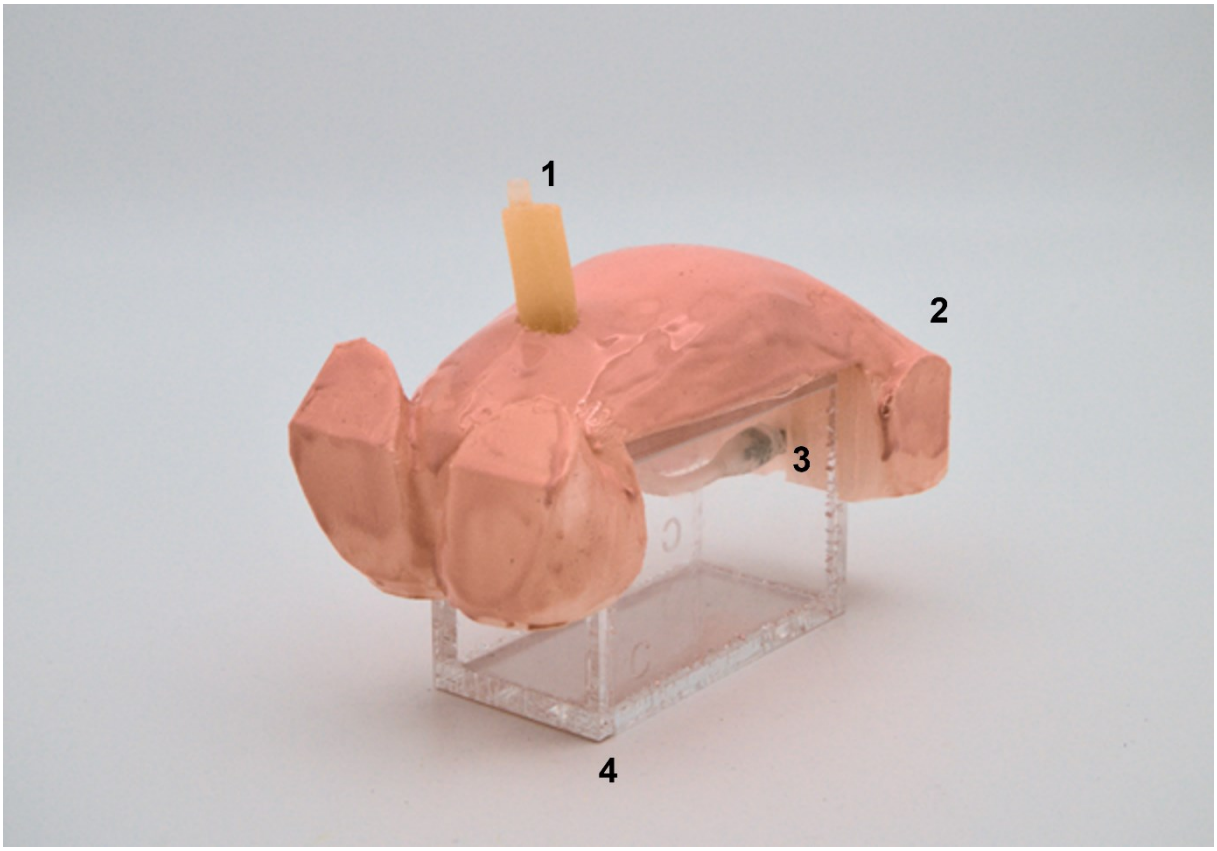

Figure Annex B.4-1: Completed setup. **1** umbilical structure consisting of Wharton jelly and vein. **2** outer shell. **3** connection point of the umbilical vein. **4** PMMA box.

Annex C Survey Questions

See document: /Annex/Annex_C_Questionnaire.pdf

Annex D Survey Results

D.1 Section 1 Consent

All participants provided consent for use of the collected data as well as video recording.

D.2 Section 2 Demographic

The demographic consisted of an even distribution of males and females, see Figure Annex D.2-1.

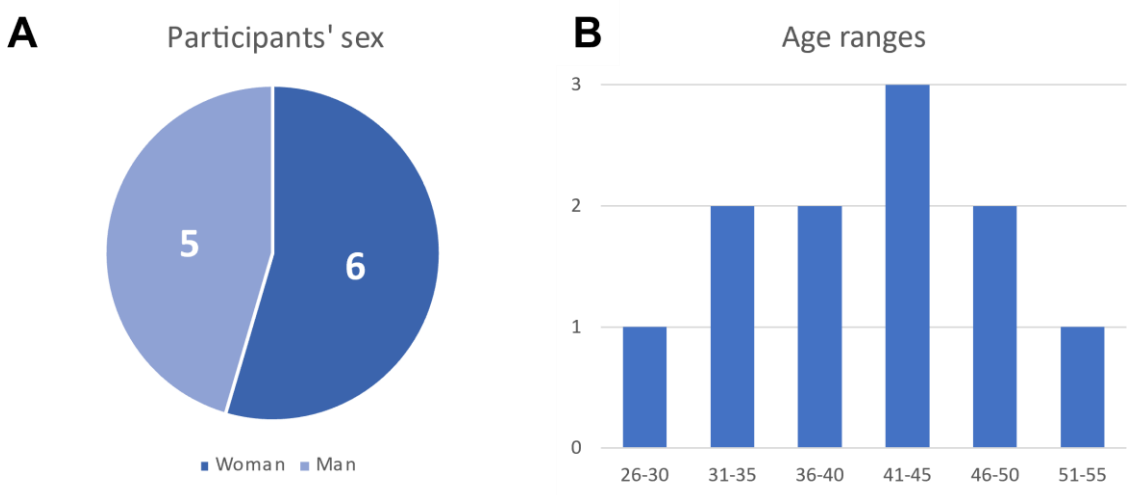

Figure Annex D.2-1: Demographic of participants who completed the entire survey. **A:** Sex distribution. **B:** Age distribution.

D.3 Section 3 Experience

Most of the participants were experienced neonatologists, see Figure Annex D.3-1. All participants answered at least either neonatologist or paediatricians.

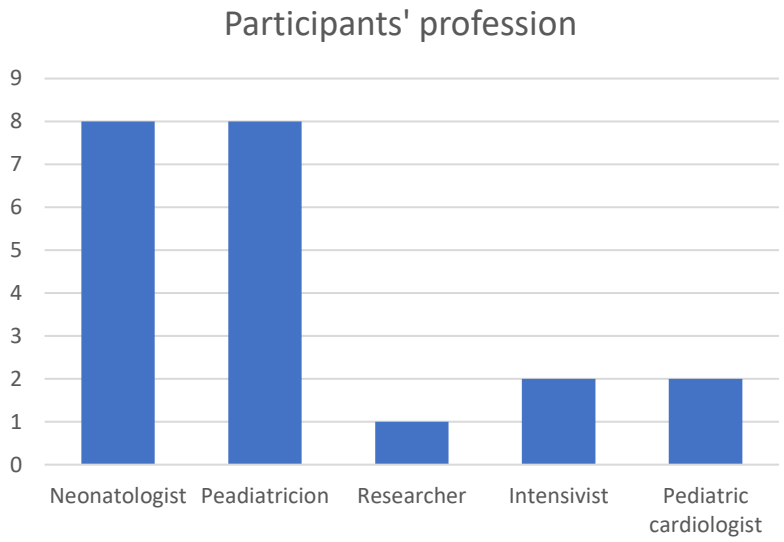

Figure Annex D.3-1: Profession of participants.

When asked to guess the number of cannulation they had performed in total, most answered around a hundred. The last 12 months, most had done around 10, see Figure Annex D.3-2.

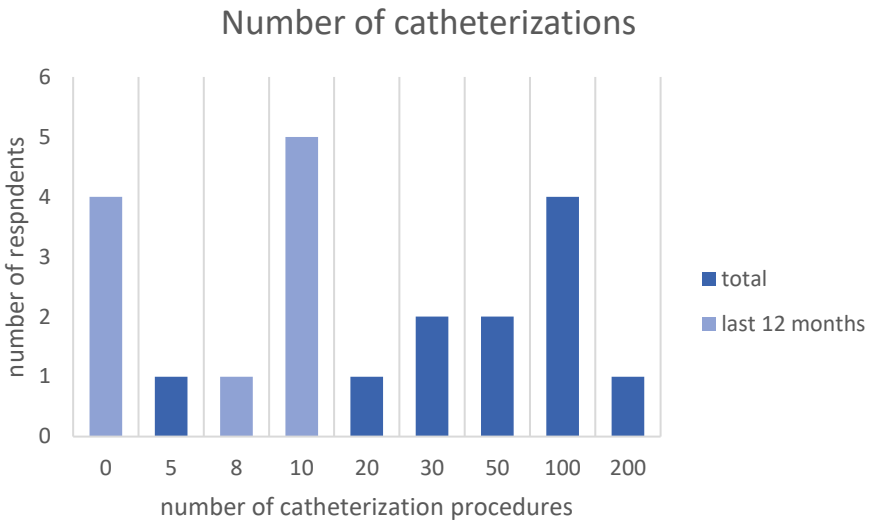

Figure Annex D.3-2: Number of cannulation procedures performed.

Most were not able to answer which size of cannula they often used, though said it was similar to the provided catheter of size 4 Fr.

Most often mentioned goals of catheterization were nutrition and medication, as represented in Figure Annex D.3-3.

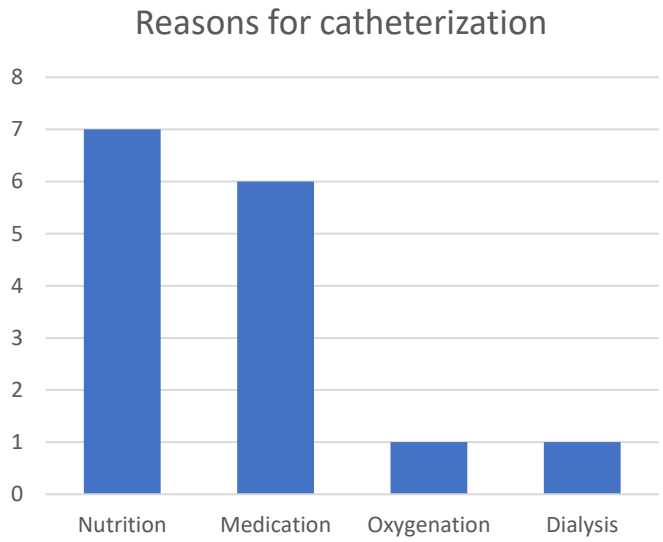

Figure Annex D.3-3: Provided reasons for catheterization.

D.4 Section 4 Training experience

Most respondents said they had had either no training at all, or training was limited to theoretical training only. One had trained on a physical synthetic simulator, see Figure Annex D.4-1 Further questioning made clear this synthetic training simulator consisted of a Laerdal Medical Umbilical Cord.

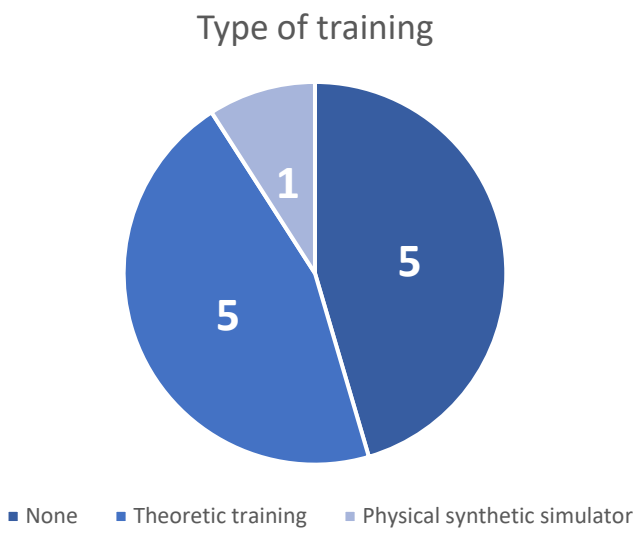

Figure Annex D.4-1: Type of training experience.

D.5 Section 5 Umbilical cord

The umbilical vein made of silicone (HT 33) was consistently ranked next to the Real UV in terms of compliancy. In terms of roughness, silicone still came closest to the Real UV on average, though not in all cases, see Table Annex D.5-1.

Table Annex D.5-1: Average distance to the ranking position of the sample with respect to the Real UV. Data is represented as mean ± std. Maximum distance is three, minimum distance is one.

Sample	Compliancy	Roughness
Vascuflex	2.55 ± 0.50	1.91 ± 0.79
Superflex	2.09 ± 0.67	2.09 ± 0.79
Silicone	1.00 ± 0.00	1.45 ± 0.66

The results of the Likert scale questions with respect to compliancy and roughness of the Wharton jelly are presented in Figure Annex D.5-1 as a stacked bar chart. Most respondents said it should neither become more stiff nor more rough, but that it should become more compliant and more slippery.

When taking applying a value of 2 for strongly agree, 1 for agree, -1 for disagree, and -2 for strongly agree an average score for each of the 4 options can be calculated. Subtracting the negative (more rough, more stiff) from the positive (more slippery, more compliant) a total score can be calculated.

This results in a score of 1.36 for more compliant and a score of 1.18 for more slippery on a scale of -2 to 2.

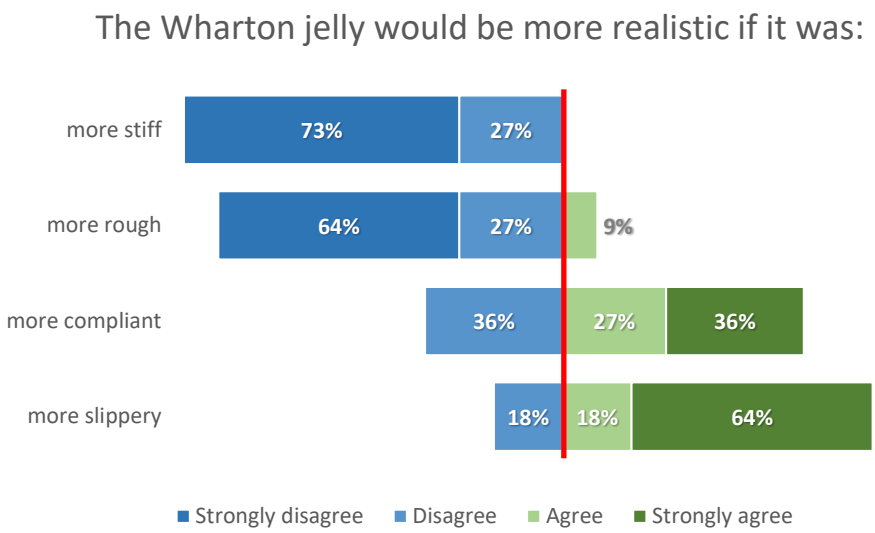

Figure Annex D.5-1: Results of the Likert scale question regarding improvement in realism of the Wharton jelly. The red line represents the neutral line.

D.6 Section 6 Cannulation procedure

Boxplots of the results show the position the materials were ranked at varied wildly between participants, show in Figure 5-8.

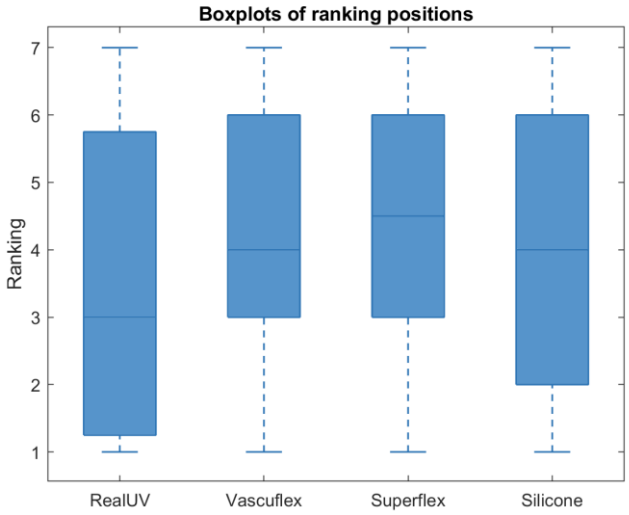

Figure Annex D.6-1: Box and whisker plots showing the spread of the different positions the materials were ranked as. Whiskers are according to Tukey's method.

The question regarding vein movement was mostly left unanswered because most participants said this was impossible to feel. The average of distance to the position of Real UV can once again be calculated, these are presented in Table Annex D.6-1. Take note that each of the materials was include twice in the ranking.

To show the difference in ranking between the same materials, the distance without taking the absolute value was calculated as well. A negative value would indicate it was ranked below the Real UV, meaning it was perceived as having less resistance. These values are presented in Table Annex D.6-2. Most are ranked on average to have less resistance compared to the Real UV. Only

Setup B (Superflex) is perceived to have more resistance than the Real UV. Though it is also in stark contrast with its counterpart Setup C. Their difference in mean position is larger than between the others.

Table Annex D.6-1: Distance in ranking with respect to cannulation resistance to the Real UV. Data are presented as mean of absolute difference ± std. Maximum distance is 5, minimum distance is 1.

Sample	Cannulation resistance ranking position
Vascuflex	2.32 ± 1.39
Superflex	2.55 ± 1.44
Silicone	3.50 ± 1.56

Table Annex D.6-2: Distance in ranking for each individual setup. Data are represented as average distance ± std. Maximum distance is 5, minimum distance is 1.

Material	Sample	Cannulation resistance ranking position
Vascuflex	Setup A	- 0.91 ± 2.11
	Setup E	- 1.18 ± 2.82
Superflex	Setup B	0.27 ± 2.89
	Setup C	- 1.00 ± 2.76
Silicone	Setup D	- 0.46 ± 3.94
	Setup F	- 0.56 ± 3.65

D.7 Section 7 – 9 Puncturing and Tearing

With regard to puncturing and tearing the results are presented in Figure Annex D.7-1: Results from the Likert scale questions regarding puncturing and tearing. Total length of each blue bar is 100%. Left of the red line corresponds to negative responds, to the right corresponds to positive responses.. Once again combining the results of both the positive and negative questions result can result in a total score for “easier to puncture” and “easier to tear”.

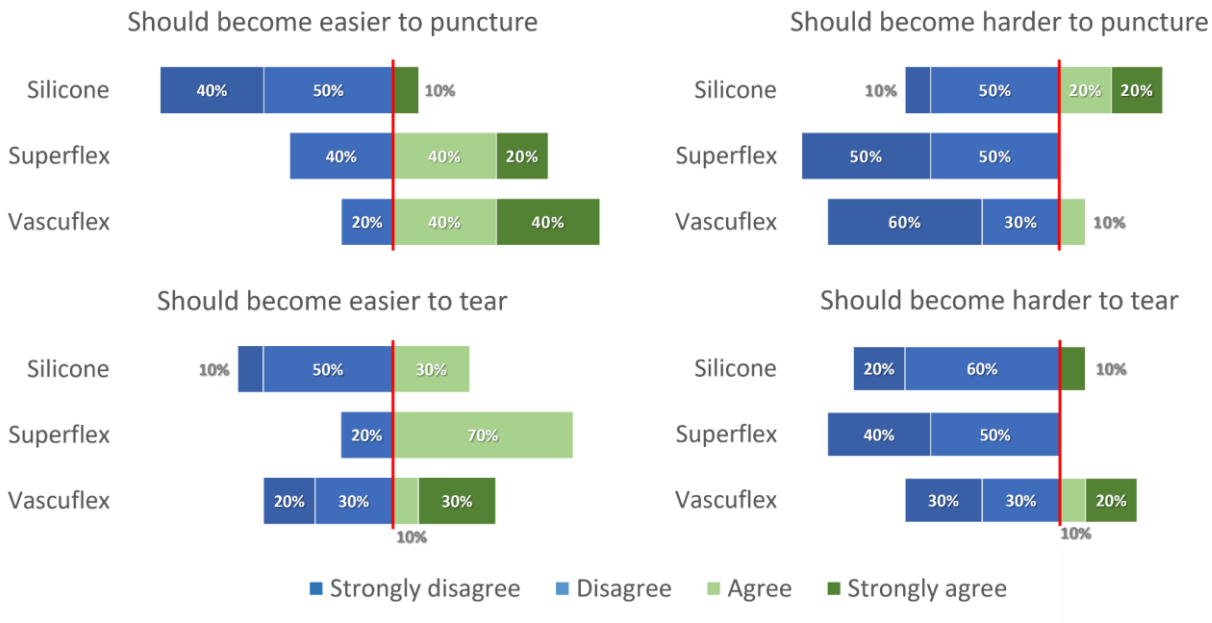

Figure Annex D.7-1: Results from the Likert scale questions regarding puncturing and tearing. Total length of each blue bar is 100%. Left of the red line corresponds to negative responds, to the right corresponds to positive responses.

These scores are presented in Table Annex D.7-1. All materials should become easier to tear. Both Vascuflex and Superflex should become easier to puncture. Only the silicone should become harder to puncture according to the participants.

Table Annex D.7-1: Total score for tearing and puncturing.

Sample	Should become easier to tear	Should become easier to puncture
Vascuflex	0.36	2.18
Superflex	1.64	1.73
Silicone	0.36	- 0.91

Annex E Creating 3d model

To obtain a 3D model of the neonate, two individual models were combined.

E.1 Scaling

The original 3D model of the venous tract was scaled down to the size of a neonate. According to literature the diameter of the VC of a neonate is around 4.2mm. Measured diameter of the inferior VC in the provided 3D model was 18.61 mm. As such, the entire model was scaled by 0.2x. Scaling was done using SolidWorks 2023 (Dassault Systèmes SolidWorks Corp.). Before importing into SolidWorks, the model was decimated using Blender with the decimate modifier at a factor of 0.2 and exported as STL.

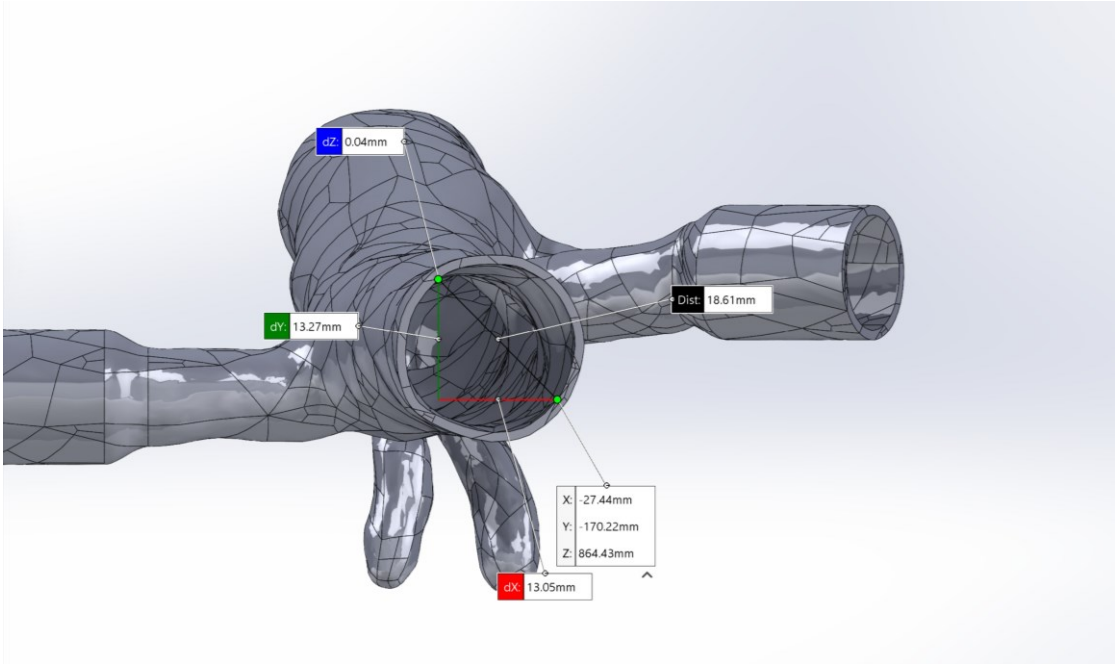

Figure Annex E.1-1: Diameter of the inferior vena cava in the model Seija van Lochem created.

E.2 Proportions

To get the proportions right, the model provided by Klinikum Nürnberg (Campus Süd) was compared with the scaled venous tract in the areas specified in Figure Annex E.2-1. Ultimately the suprarenal and infrarenal portion of the vena cava were chosen to lengthen. This resulted in the lengthening factors presented in Table Annex E.2-1. Measurements were done in Blender 3.4 (Blender foundation). Extending was done in SolidWorks 2023 (Dassault Systèmes SolidWorks Corp.).

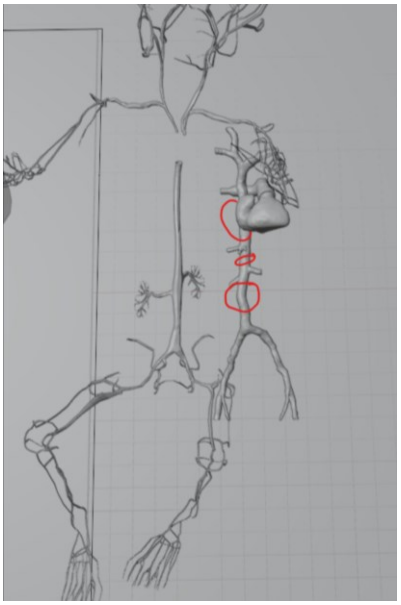

Figure Annex E.2-1: Areas changed to obtain correct proportions.

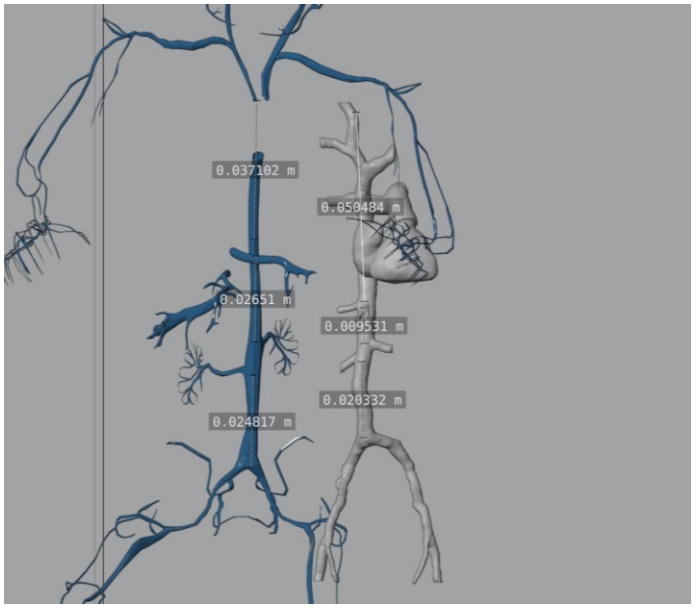

Figure Annex E.2-2: Measurements of the vena cava in a neonate and the scaled down model of an adult.

Table Annex E.2-1: Fractions for the intrarenal and suprarenal portion of the vena cava. Measurements are shown in mm.

Areas	fraction	factor
Infrarenal	0.0265/0.0095	2.79
Suprarenal	0.0248/0.0203	1.22

E.3 Combining the models

To obtain a venous tract including umbilical vein, the 3D model provided by Klinikum Nürnberg (Campus Süd) was combined with the downscaled adult model. The model of the UV was shaped after an x-ray of guide wires while inserted into umbilical veins.

First, the previously downscaled model was imported into Blender. Then the umbilical vein, visible in pink in Figure Annex E.3-1, was extracted from the provided model and imported into Blender twice, overlayed onto each other. To combine the two models, two Boolean operations were performed. This was necessary to make sure the two veins intersected correctly.

Connection angle was based on the angle as found in the provided 3D data.

The combined model is shown in Figure Annex E.3-2.

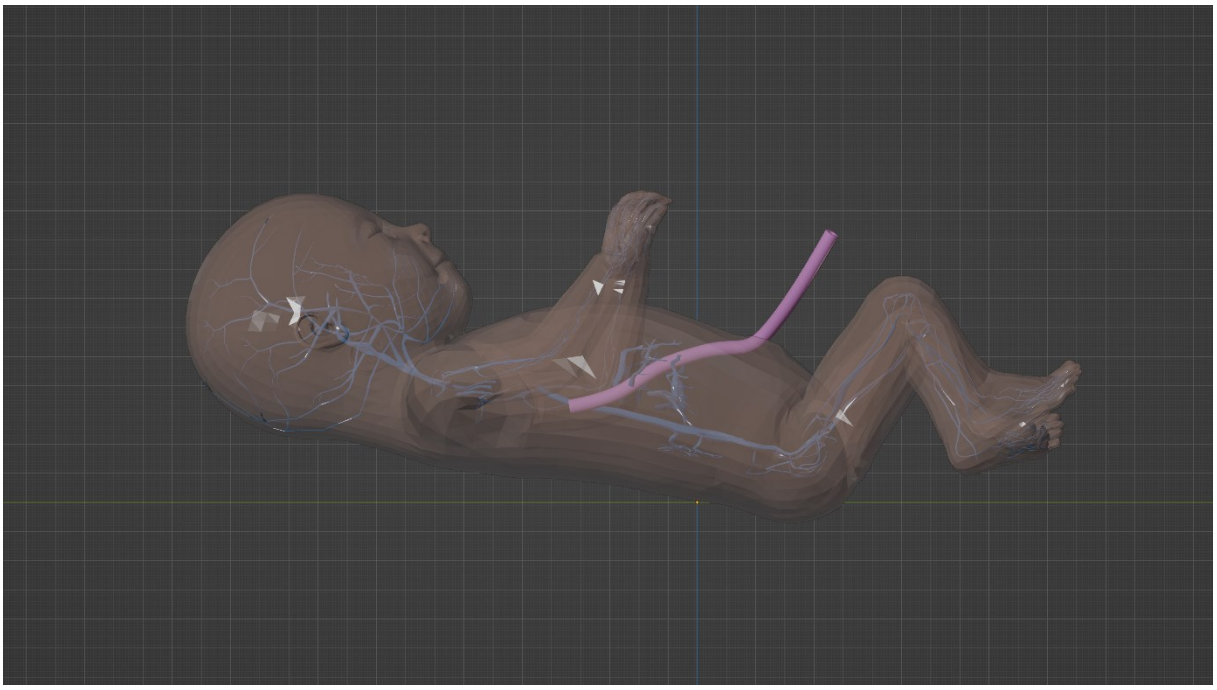

Figure Annex E.3-1: The 3D model provided by Klinikum Nürnberg (Campus Süd). In pink the UV as recorded from x-ray images.

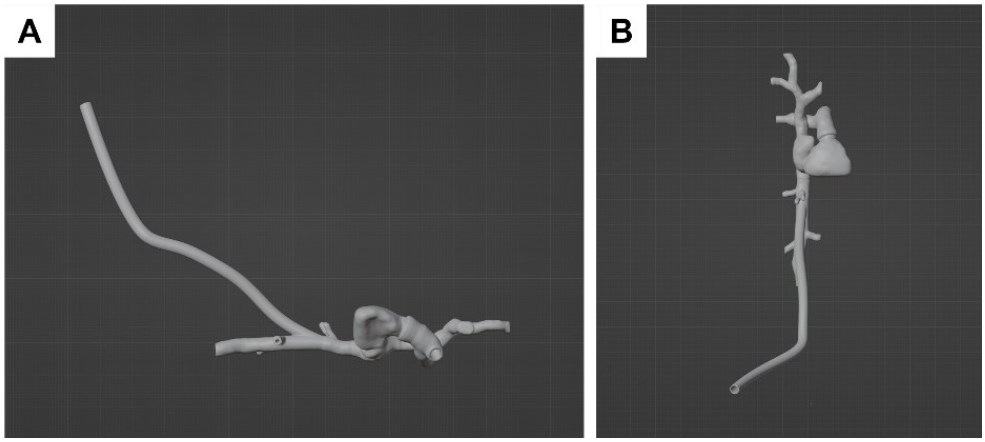

Figure Annex E.3-2: Resulting 3D model of the neonates' venous tract. A: lateral view. B: frontal view.

E.4 Adding connectors

To make sure the venous tract could be connected to a pump system, to each of the openings a connector was added. For details see Figure Annex E.4-1.

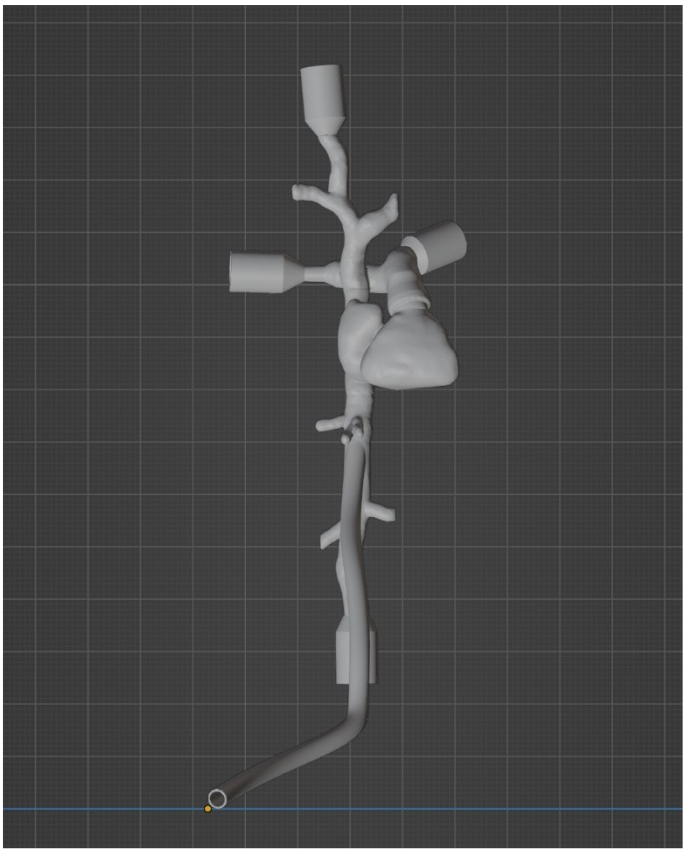

Figure Annex E.4-1: Full connected model including umbilical vein and connectors for connecting to water supply.

Annex F User Requirements Specification

See document: Annex/Annex_F_URS_1311023LWd.docx

Annex G Additional Statistical analysis

G.1 Mann-Whitney-U-test

Even though the Shapiro-Wilk test came out insignificant, sample sizes were still very small which makes the Shapiro-Wilk test unreliable. HUV consisted of only three samples, Dragon Skin 20 of eight, and all other materials of just five. Therefore, additionally a non-parametric Mann-Whitney U-test was caried out.

The results are present in Figure Annex G.1-2.

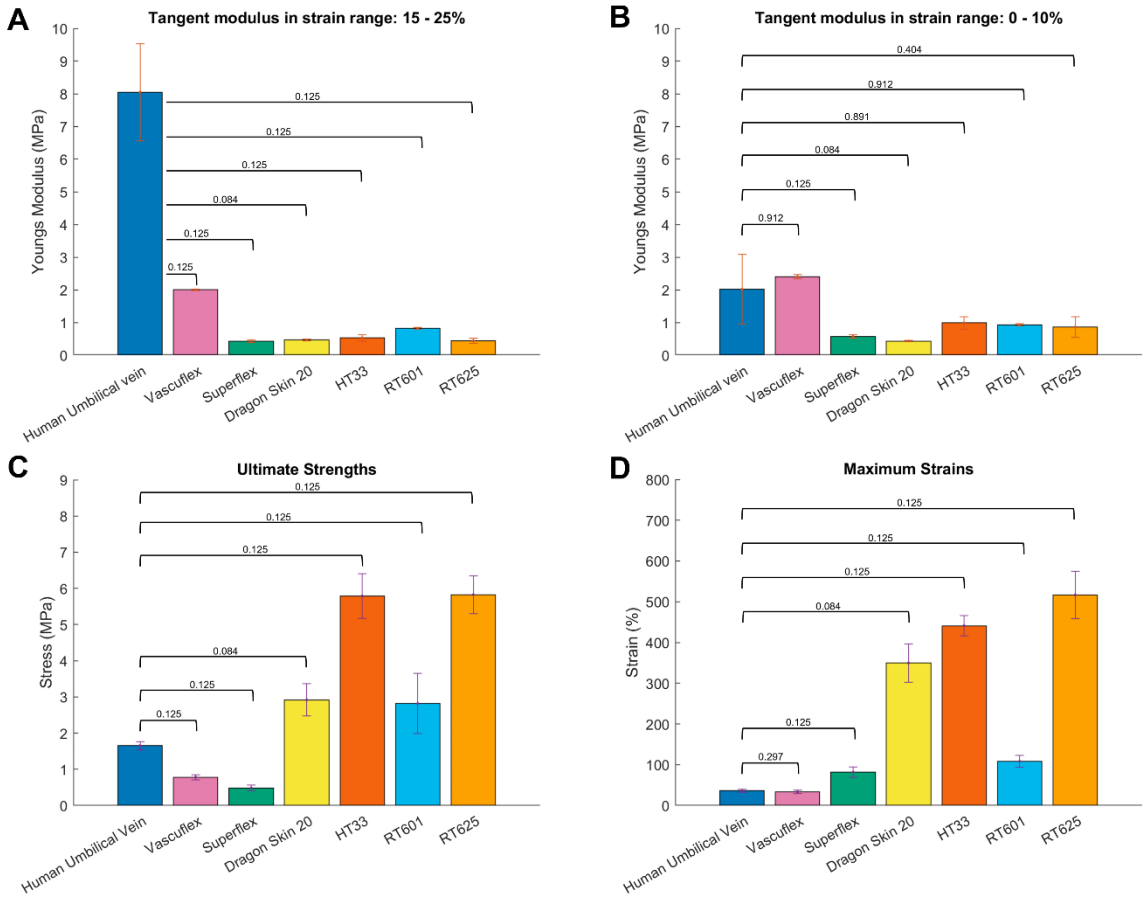

Figure Annex G.1-1: Bar charts containing mean and standard deviations from extracted mechanical parameters. p-values for the Mann-Whitney-U-test in comparison to HUV are indicated after the Holm-Bonferroni correction. **A:** Tangent moduli for the part where HUV behaves linearly. **B:** Tangent moduli on small strains. **C:** Ultimate strengths. **D:** Maximum strains.

At $\alpha = 5$ %, none of the materials are deemed statistically significantly different in any of the four properties. However, a U-statistic of 0.000 was found for all materials in terms of tangent modulus in strain range 15 – 25 %. A U-statistic of 0.000 usually indicates there is no overlap in values between two groups. All values of either group are thus higher than all values of the other group. This should give a strong indication that both do not belong to the same population or, in case of the Mann-Whitney-U-test, a very low p-value.

It is likely that the combination of a low sample size and the application of Holm-Bonferroni pushes the p-values above 0.05.

To give an indication of this behavior, Figure Annex G.1-2 is included. All materials lie between 0 and 2 MPa, while HUV lies around 8 MPa.

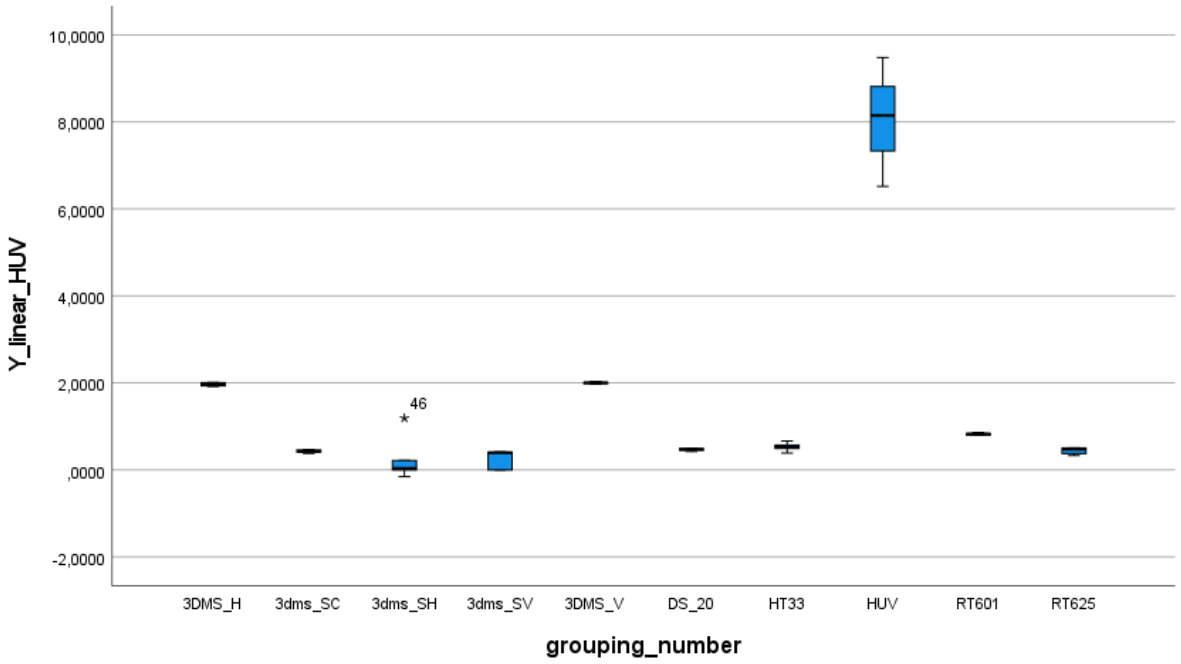

Figure Annex G.1-2: Box-plots for the samples regarding the strain range for which HUV behaves linearly.

Annex H Alternative materials

Material	Technique	Mechanical properties			Price indication / availability
		ε_{break}	UTS	Shore A	
TissueMatrix [1]	PolyJet 3D printing using Stratasys Objet 3D printers.				Requires specialized printer
TangoPlus FullCure 930 [2]	PolyJet 3D printing using Stratasys Objet 3D printers.				Requires specialized printer
SIL-001	Direct Silicone 3D printing by Lynxter [3]. Two-part silicones are mixed in the nozzle and only fully cured after printing.	300%	N/A	50	Printer available at the Saxion FabLab. Small print (neonate venous tract) costs "hundreds of euro's". Availability: since March 2024
SIL 30	Two-part silicone printing by Sandraw [4], using Fluid Additive Manufacturing (FAM). With new support material, smaller vessels are possible.	900%	9.7 MPa	30	Available from China, Quote for the provided 3D-model (neonate venous tract): $244 Availability: since end of April 2024
Natural rubber [5]	Coating	100-800%	28 MPa	30-100	Widely available

[1] "TissueMatrix Soft and contractile." https://www.stratasys.com/en/materials/materials-catalog/polyjet-materials/tissuematrix/ (accessed 17-06-2024, 2024).

[2] J. Garcia, M. AlOmran, A. Emmott, R. Mongrain, K. Lachapelle, and R. Leask, "Tunable 3D printed multi-material composites to enhance tissue fidelity for surgical simulation," *Journal of Surgical Simulation,* vol. 5, no. 1, pp. 87-98, 2018, doi: 10.1102/2051-7726.2018.0013.

[3] "Lynxter, CUSTOMIZED PRODUCTION LIMITLESS MATERIALS." https://lynxter.fr/en/ (accessed 06-06-2024, 2024).

[4] "Sandraw." https://www.sandraw.com/ (accessed 06-06-2024, 2024).

[5] "Natural Rubber, Vulcanized (NR, IR, Polyisoprene)." https://www.matweb.com/search/datasheet.aspx?matguid=6588439546ac4492965c894ddff3f5da&ckck=1 (accessed 17-06-2024, 2024).